Spring 5-15-2024

STRUCTURAL AND THERMOMECHANICAL PROPERTIES OF RIGID POLYURETHANE FOAMS PREPARED USING FRESH AND RECYCLED CANOLA OIL

Janu Patel
Pittsburg State University, januashokkumar.patel@gus.pittstate.edu

Recommended Citation
Patel, Janu, "STRUCTURAL AND THERMOMECHANICAL PROPERTIES OF RIGID POLYURETHANE FOAMS PREPARED USING FRESH AND RECYCLED CANOLA OIL" (2024). *Electronic Theses & Dissertations*. 520.
https://digitalcommons.pittstate.edu/etd/520

STRUCTURAL AND THERMOMECHANICAL PROPERTIES OF RIGID POLYURETHANE FOAMS PREPARED USING FRESH AND RECYCLED CANOLA OIL

Thesis Submitted to the Graduate School
in Partial Fulfilment of the Requirements
For the Degree of
Master of Science

Janu A. Patel

Pittsburg State University

Pittsburg, Kansas

May 2024

STRUCTURAL AND THERMOMECHANICAL PROPERTIES OF RIGID POLYURETHANE FOAMS PREPARED USING FRESH AND RECYCLED CANOLA OIL

Janu A. Patel

APPROVED:

Thesis Advisor ______________________________
Dr. Ram K. Gupta, Department of Chemistry

Committee Member ______________________________
Dr. Khamis Siam, Department of Chemistry

Committee Member ______________________________
Dr. Anuradha Ghosh, Department of Biology

Committee Member ______________________________
Dr. John Franklin, Department of English and Modern Languages

Acknowledgments

I would like to express my profound gratitude to all whose contributions have culminated in completing this thesis. Foremost among them is Dr. Ram K. Gupta, whose guidance and support have been indispensable throughout my pursuit of a master's degree in polymer chemistry. Dr. Gupta has served as my teacher and research advisor and has been a constant source of motivation, empowering me to strive toward my academic aspirations. His knowledge and extensive experience have been instrumental in shaping my research endeavors in the right direction. I am deeply grateful for Dr. Gupta's time and effort in reviewing and advising on my work and refining it into a comprehensive piece.

I extend my heartfelt appreciation to Dr. Khamis Siam, Dr. Anuradha Ghosh, and Dr. John Franklin for their invaluable contributions as members of my thesis committee and for offering indispensable insights that have shaped the direction of my research. I am grateful for the generous support provided by the National Institute for Materials Advancement, the Department of Chemistry, and Pittsburg State University through financial assistance and scholarships, which have enabled me to pursue my academic endeavors. Furthermore, I am indebted to Dr. Peter Dvornik, Dr. Jeanne Nortan, and Mr. Paul Herring for teaching me in-depth polymer chemistry. My heartfelt thanks are also extended to my family for their unwavering encouragement, love, and understanding throughout the challenges of this academic journey. Their belief in my abilities has served as a constant source of motivation and strength. I am grateful to my friends and peers for their academic and emotional support. Their encouragement and friendship have created a positive and enjoyable environment in which I have thrived.

STRUCTURAL AND THERMOMECHANICAL PROPERTIES OF RIGID POLYURETHANE FOAMS PREPARED USING FRESH AND RECYCLED CANOLA OIL

An Abstract of the Thesis by
Janu A. Patel

Polyurethane (PU) is a versatile and widely utilized polymer with a broad spectrum of applications across various industries. Its unique properties make it suitable for numerous products that enhance comfort and efficiency in everyday life. Traditional PU production relies on petroleum-based raw materials, which have negative impacts on the environment. This study focuses on the utilization of waste cooking oil (WCO), specifically three to four times-used canola oil (UCO), to synthesize rigid polyurethane foams (RPUFs) as an environmentally friendly alternative by replacing petroleum-based raw materials. This approach also aims to address environmental concerns associated with the improper disposal of WCO into drainage systems, land, and rivers and reduce dependence on costly fresh vegetable oils for PU production. WCO is readily available as a byproduct of domestic cooking, food service establishments, and industries. In this work, UCO was collected from domestic sources, filtered, and converted into polyol, which serves as a key component in producing RPUFs, using epoxidation and ring-opening methods. The quality of UCO-based polyol was compared with polyol synthesized from new canola oil (NCO) through qualitative tests including the iodine test, epoxy-oxirane oxygen test, Fourier transform infrared (FTIR), hydroxyl number analysis, and so on. The fire resistivity of RPUFs was also tested by introducing flame retardants such as dimethyl methyl phosphonate (DMMP) and expandable graphite (EG). The final synthesized material was tested to assess properties like fire retardancy, thermal stability, and cell structure of RPUFs. DMMP-contained foam lost its weight by 12.10% and burned for 8.3 seconds instead of 54.9 seconds in pure PU foam. EG-treated foam also demonstrated advantages in flame retardancy with a weight drop of 5.86% and a burning period of only 16.5 seconds. The closed-cell content of all the foams was above 90%, which is a crucial characteristic for foam insulation applications. The results indicate that UCO can be effectively utilized for producing high-quality RPUFs. This suggests the potential for using WCO as a sustainable and cost-effective raw material in PU foam manufacturing.

TABLE OF CONTENTS

LIST OF TABLES

LIST OF FIGURES

LIST OF ABBREVIATIONS

ASTM	American Society for Testing and Materials
CCC	Closed Cell Content
CO	Carbon Monoxide
DMMP	Dimethyl Methyl Phosphonate
DTGA	Derivative Thermogravimetric Analysis
EG	Expandable Graphite
ENCO	Epoxidized New Canola Oil
EUCO	Epoxidized Used Canola Oil
FPUF	Flexible Polyurethane Foam
FR	Flame Retardant
FT-IR	Fourier-Transform Infrared Spectroscopy
GPC	Gel Permeation Chromatography
HCN	Hydrogen Cyanide
MDI	Methylene Diphenyl Diisocyanate
NCO	New Canola Oil
NCOP	New Canola Oil Polyol
PU	Polyurethane
RPUF	Rigid Polyurethane Foam
RT	Room Temperature
SEM	Scanning Electron Microscope
TDI	Toluene Diisocyanate
TGA	Thermogravimetric Analysis

UCO	Used Canola Oil
UCOP	Used Canola Oil Polyol
WCO	Waste Cooking Oil

CHAPTER I

INTRODUCTION

1.1. Polymer

Polymers are large molecules composed of multiple repeating components referred to as monomers. A few synthetic polymers were developed in the early 1900s, and the following years saw the discovery of polyvinyl chloride (PVC, 1931), polyethylene (PE, 1933), polyvinylidene chloride (Saran, 1933), polyamides (nylon, 1934), and polytetrafluoroethylene (Teflon, 1938), each of which contributed to the rapid rise of polymer science. In addition, polystyrene (PS), polyurethane (PU), and ethyl vinyl acetate (EVA) are some examples of polymers that are widely used in the building and construction sectors [1,2].

1.1. Polyurethane: Overview & Background

PUs have been one of the most commonly used groups of polymers in the world in recent years [3]. Wurtz produced urethane for the first time in 1849 [4]. Carother's work at E.I. Dupont resulted in the invention of high molecular weight polyamides (nylons) which encouraged Dr. Bayer to create a comparable compound [5]. Initially, the reaction between aliphatic isocyanate and diamine yielded polyurea, which is infusible and hydrophilic. Later investigation revealed that the interaction of an aliphatic isocyanate and a glycol produced a novel molecule [5]. At the I.G. Farben laboratory in Leverkusen, Germany, in 1937, Dr. Otto Bayer and his colleagues discovered PU through the polyaddition reaction between a polyester diol and a diisocyanate in the presence of a catalyst, chain extender, and other additives [4,6].

PU has numerous uses in industries, including adhesives, coatings, flexible and rigid foams, elastomers, and many more [7]. These uses are made possible by the exceptional qualities of PU, which include low density, low moisture absorption, low thermal conductivity, lightweight, and so forth [8]. Because of those qualities, PU is employed in many other applications, including insulating panels, footwear, energy absorption, bedding, aircraft, automotive components [9], packaging, and medical equipment [10]. Owing to the superior properties of PUs, the US government has replaced chlorinated rubber with PU in the marine and aircraft industries, as chlorinated rubber includes unstable organic chemicals that are detrimental to the environment [11]. Similarly, PU foams have overtaken latex rubber in the auto production industry for interior cushioning and automobile seats because of their greater flexibility and reduced density [11].

1.3. Chemistry of Polyurethane

PU is typically produced by reacting -OH group of polyols with -NCO group of isocyanates [12,13]. The word polyurethane comes from the urethane linkage found in the PU [4]. Water is commonly utilized as a blowing agent, which produces CO_2 gas when it reacts with isocyanate groups. Therefore, to control the morphology of the cell structure of the foams, isocyanate, and polyol, along with surfactants, blowing agents, and catalysts, are employed [14]. The physical and chemical characteristics of PU are influenced by the structure and proportion of polyol and isocyanate used throughout the synthesis process

[15]. Long, flexible segments of polyol can generally be used to create soft elastic polymers, but more cross-linking and shorter chains are needed to create rigid polymers [16]. The isocyanate reaction plays an important role in understanding the chemistry of PUs [5]. Isocyanate is a strained linear molecule, which has two accumulated double bonds N=C and C=O [17]. It is a reactive compound that interacts with -OH and -NH functional atoms to form a variety of chemically distinct products. Isocyanate incorporates the hydroxyl group to form urethane molecules, whereas urea molecules are generated by the reaction with the amine group [5]. The aliphatic diisocyanate generated from dimerized fatty acids has limited reactivity for foam applications, but it can be used for coatings and other urethane applications. Consequently, aromatic diisocyanate is required to produce foams [18].

1.4. Classification of Polyurethane

Simply classifying PU is challenging due to its widespread use in various fields. Consequently, PU is categorized according to its type, raw material, and thermal response as shown in **Figure 1**.

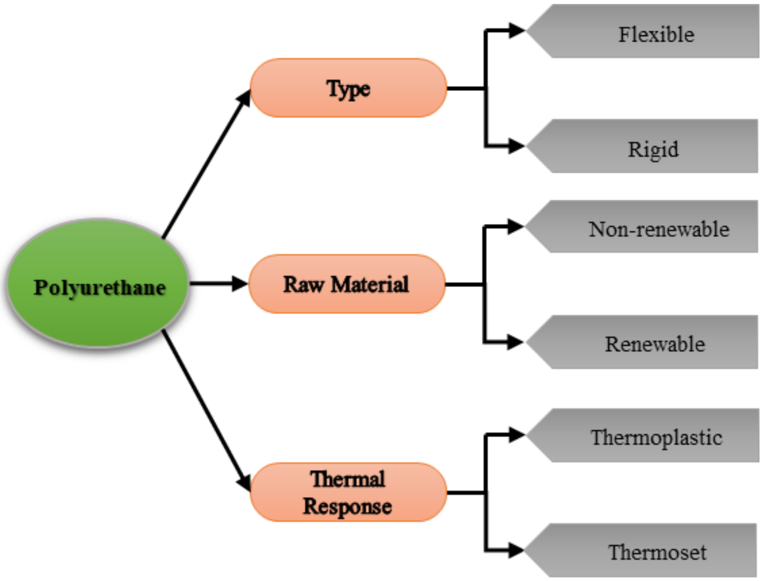

Figure 1. Classification of polyurethane.

1.4.1. Types of Polyurethane

1.4.1.1. Flexible Polyurethane Foam

Flexible polyurethane foams (FPUFs) are block copolymers having elastic attributes resulting from the phase separation of "hard blocks" and "soft blocks.” Hard blocks are rigid structures, that are physically cross-linked and which deliver firmness to the polymer, while soft blocks are stretchable chains providing elasticity to the polymer [19]. Comparable to a coiled metal spring, FPUs exhibit low-bearing and higher recovery properties. FPUs have an open-cell structure that allows air to easily circulate throughout the material. In the manufacturing sectors such as furniture, carpet, packaging, machinery, and bedding, FPUs are indispensable [20].

1.4.1.2. Rigid Polyurethane Foam

Rigid polyurethane foams (RPUFs) have been significantly utilized in thermal insulation and the building sectors because of their qualities for products such as thermal insulation and mechanical properties, which rely on the thickness of the cell wall, cell shape, and size distribution, among other aspects of their structure. The potential for heat absorption is also developed by trapping air inside the cellular structure resulting in thermal insulating properties. RPUFs have low thermal conductivity and high mechanical and chemical stability at both high and low temperatures [14,21]. RPUFs have good resistance, high strength, and low weight characteristics. Moreover, with increasing density the strength of RPUF rises, and with increasing temperature it falls. In RPUF, the proportion of closed cell content depends not only on the degree of crosslinking and the surfactant (taken at the time of production) but also on the equivalent weight of polyol [20].

1.4.2. Raw Materials

To create PU, a polyol is reacted with isocyanate; the polyol is mainly obtained from petroleum-based resources [22,23]. Petroleum-based polyurethanes are not ecologically friendly, are expensive for technology processing systems, and are non-renewable [22]. Furthermore, looking for biobased alternatives is necessary due to the considerable greenhouse gas emissions and enormous heat consumption of petroleum-based products during processing, as well as the shortage of raw materials and environmental regulations [24]. Among biobased resources, vegetable oils containing triacyl glycerides have the potential to be used as a starting material in the formation of PU [25–28]. In this scenario, replacing non-renewable PU feedstock with renewable vegetable oil, such as soybean oil, rapeseed oil, palm oil, peanut oil, cotton oil, and sunflower oil, is worthwhile [29]. Moreover, cork, starch, liquefied lignin, coffee grounds, date seeds, and sugar beet pulp are added during the creation of PUs rather than petroleum-based materials, and resulting components have similar density, thermal conductivity, and cellular morphology in foams to those produced using fossil fuels [14].

1.4.3. Thermal Response

In general, thermoplastic, and thermoset PU are two distinct groups of synthetic PU polymers [15,30]. PUs comprising difunctional components are thermoplastic; on the other hand, thermosets have molecules with tri- or multifunctional components that cause the material to cross-link chemically [15]. Linear polymer compounds are found in thermoplastics; these compounds can be reshaped by heating, and they can be melted and solidified without undergoing any chemical changes. This indicates that a limited amount of heating and cooling cycles can be carried out without causing any structural or functional modifications, such as changes in color and shape, microstructural alterations, or mechanical dysfunction. Thermosets are cross-linked polymers that disintegrate under heat but do not melt [30,31]. Thermoset PU forms interconnected networks because of the cross-linked polymer, which gives rise to a hard and rigid product. Consequently, heating the thermoset polymer will cause structural modification and chemical breakdown. Thermoplastic materials are usually temperature-dependent, while thermosets are not. The thermoplastic polymer will be glassy and brittle when the glass transition temperature (Tg) is above room temperature (RT), whereas Tg close to RT yields thermoplastic PU that is less rigid and tougher. Thermoplastic and thermoset PUs exhibit enormous potential for developing modern manufacturing. High molecular weight thermoplastics have excellent mechanical qualities such as chemical stability, optical transparency, self-lubrication ability, and hydrophobicity, which make them ideal for use in molded items, fibers, films, and adhesives. Thermosets have similar applications but are less useful as fiber [31,32].

1.5. Applications of Polyurethane

Since its creation, PU has been employed in a wide range of areas, including adhesive, synthetic leather, coating and elastomer, because of its superior properties, such as flexible formulation, high product performance, and a variety of foams [7,33]. Additionally, PU is also used in industries like packaging, medicine, footwear, paint, and coating [34].

PU foam has found widespread application in impact absorption devices, the aerospace and automobile industries, as well as in biomedical applications, owing to its unique features, including a cellular structure, low density, and high energy absorption capacity [35]. Additionally, because of these characteristics, it is also utilized in thermal insulation panels that cover the insulation in walls and roofs and in space for stuffing around windows and doors [33]. However, several aspects influence the chemical and physical properties of PU foams: namely, crosslinked density and flexibility; functional group; as well as the effect of isocyanate and polyol, and their concentrations [20]. For instance, PU foams based on polyether are a softer and more favorable material when comfort is the main priority. This particular kind of foam serves applications for cushioning, carpet underlay, furniture, pillows, and bedding. On the other hand, polyester-based PU foam is heavily used for shoulder pads, acoustic, textiles, and other purposes [36].

1.6. Issue with Polyurethane Foams

The use of RPUFs is limited due to their high flammability. RPUFs are combustible that quickly spread flame and have high heat release rates [37–39]. RPUFs are composed of porous cellular structures that increase contact between the substance and air. Because of this, RPUFs emit dangerous fumes that include carbon monoxide (CO), hydrogen cyanide (HCN), NH_3, NOx, and many other toxic gases during combustion [40,41]. The smoke from burning PU foams harms people's health and may even cause death, and it also adversely affects the environment. In the fire environment, CO generated from flame and smoldering combustion is regarded as an extreme danger. CO from smoldering is a very complicated combustion phenomenon that is hard to comprehend in terms of chemistry and physics [42,43]. HCN is formed immediately following fire since PU contains a large amount of nitrogen in its structure. Because of the high concentration of isocyanate in the PU chain, it generates more HCN than other nitrogen-containing polymers, such as nylons and polyacrylonitriles. Most of the heat, CO_2, and CO emissions are caused by the burning of the polyol [44].

The harmful effects of smoke in PU combustion can be classified into three categories. First, the ignited smoke of PU contains several harmful substances, including CO, HCN, and many more, that may cause poisoning and suffocation. Second, high temperatures cause smoke, which has a lot of heat and can promote the development of fire. Third, fire smoke may block people's vision, which could affect rescue and evacuation efforts [42]. Therefore, the addition of flame retardant is necessary to reduce the flammability of RPUFs [40].

Aside from this, the considerable reliance of PU foams on resources derived from petroleum is another significant issue [45]. Thus, replacing these fossil fuel-based materials with renewable biobased alternatives is preferable. It not only complies with legislative criteria but also lowers production costs to obtain the required components. Renewable resources contribute to reducing problems with the environment by eliminating greenhouse gas emissions [46,47].

1.7. Polyol

Polyol comprises two or more hydroxyl (-OH) functional groups in their structure [15]. Polyol is the primary raw ingredient used to create PU [48]. The majority of industrially produced PU is typically synthesized using resources that come from petroleum. Petroleum-based products are an enemy to the environment because of their high carbon footprint, depletion of non-renewable resources, and improper disposal of waste. Thus, the goal of many researchers is to use renewable resources to replace materials that come from petroleum [34].

Protein, lignin, starch, and natural oil are a few examples of biobased raw materials, but vegetable oil has gained a lot of attention as a renewable source during the last few decades because of its lower environmental impact and the agricultural benefits of using it [34,49,50]. Vegetable oils are widely accessible, biodegradable, ecologically friendly, and non-toxic. Vegetable oil has been used to synthesize PU [34,45]. Vegetable oils are primarily composed of triglycerides, which include glycerol and three long-chain fatty acids such as stearic, oleic, palmitic, linoleic, and linolenic, depending on the oil source. Triglycerides enhance the physical and chemical properties of the PUs, like their thermal stability. The two primary structural elements found in vegetable oil are carbon-carbon double bonds and ester linkages, utilized to introduce the hydroxyl group by chemical alteration to produce polyol [34,45,48]. However, the cost of vegetable oil is high, which is why some work has gone into creating polyol for RPUFs from waste cooking oil (WCO)

[22]. There are several synthetic routes to obtain polyol, namely epoxidation and ring opening, ozonolysis, hydroformylation, esterification, acrylation, and animolysis [18,34].

Polyols can be separated into two types: polyether and polyester. Polyether polyol is created through a reaction between epoxide and an active hydrogen compound, whereas polyester polyol is manufactured through the polycondensation method, which involves the combination of multifunctional carboxylic acids and hydroxyl compounds. They can be further subdivided based on the molecular weight of the polyol. FPUFs are made from high molecular weight polyols, ranging from 2,000 to 10,000 [51]. For example, in the slabstock formulation, a polyol with around 3000 molecular weight polyether triol is employed, whereas a polyol with an approximately 5000 molecular weight ethylene oxide capped polyether triol is used in the molded foams [52].

In contrast, rigid products are produced by utilizing a lower molecular weight polyol. [51]. Since reduced demould periods are one of the main goals for the creation of the moulded foams, ethylene oxide capping had been selected over propylene oxide due to its much higher reactivity owing to the primary hydroxyl groups [52]. The compatibility, water solubility, and reactivity of polyols are influenced by the quantity of oxide and the sequence in which they are added [51].

1.8. Waste Cooking Oil

Since edible oils are more aggressively demanded in the food supply and have comparatively higher manufacturing costs, using raw vegetable oil directly may present a challenge. As a result, WCO is a sought-after, inexpensive derivative of virgin oils [53]. A substantial amount of WCO resources is produced because of the extensive utilization of vegetable oil. The United States generates more WCO than any other country, followed by

China, England, Europe, Malaysia, Japan, and Ireland [54]. Cooking oil is frequently reused, mostly by fast food sellers and in residences. Continuous usage of these oils modifies their characteristics, as evidenced by variations in the viscosity, odor, smoke point, and color of the oil. WCO is regarded as household waste material that, if improperly disposed of, could endanger the environment by contaminating drainages, water bodies, and landfills [53].

According to a survey by the Agricultural and Food Development Authority, WCO that is poured into the kitchen sink clogs 40% of the sewage line. One of the foremost environmental issues with WCO is eutrophication, which occurs when a thin layer of oil prevents sunlight from permeating the surface of a river, ultimately disrupting the provision of oxygen for aquatic life. The water quality in a lake or river is also impacted by the aquatic ecosystem's unbalanced equilibrium. The primary source of contamination in rivers is vehicle engine oil or WCO from domestic areas [54]. Apart from this, there are detrimental impacts on human health from consuming WCO. Cooking methods that involve high temperatures, like grilling or pan-frying, have been linked to a higher risk of carcinogenicity and genotoxicity [55]. In the context of environmental and health concerns, this study synthesized RPUFs using polyol derived from used canola oil (UCO) and then compared their properties to those of RPUFs based on polyol developed from new canola oil (NCO).

1.9. Isocyanate

The chemical isocyanate is stretched linear having a highly reactive isocyanate group (-N=C=O) and consists of two cumulated double bonds including N=C and C=O. It is a key ingredient in the step-growth polymerization process that yields PU by reacting with polyol and chain extenders having a small molecular weight. The rising level of PU output is the key driver of the 5% annual growth in the isocyanate market worldwide [17][56]. Toluene diisocyanate (TDI), methylene diphenyl diisocyanate (MDI), isophorone diisocyanate (IPDI), and 1,6-hexamethylene diisocyanate (HDI) are some of the common examples of isocyanate. Isocyanate can be either difunctional or polyfunctional in nature. Most isocyanates are difunctional, meaning that every molecule has two isocyanate (-NCO) groups [16]. The type of isocyanate used has a great influence on the mechanical characteristics of PU; for example, isocyanate possessing a high number of aromatic rings and methylene groups gives better tensile strength. To clarify it better, HDI has the weakest qualities due to its low reactivity, which results in a low molecular weight. Because of their greater reactivity with macro diols, TDI has a higher tensile strength and a lower strain than MDI [56].

Isocyanate groups can undergo three different reactions: interaction between isocyanate groups, resulting in the creation of two cyclic compounds- isocyanurate rings and uretidione; interaction with substances that contain active hydrogen atoms in their chain; interaction with chemical substances lacking hydrogen atoms. A polymer can be formed by any of these reactions, but the most significant one from a technological standpoint is the one that produces PU when the NCO group combines with substances that have active hydrogen atoms. From a chemical standpoint, isocyanates can be classified as either aromatic or aliphatic [56].

Aromatic or aliphatic isocyanate combining polymers have a diverse range of properties, which include density, rigidity, and flexibility; this makes them valuable for a variety of goods in many applications such as foams, paint ingredients, glue, matrixes for composites, and so on. For example, PU items that are rigid have been prepared with methylene diphenyl diisocyanate, while flexible products have been prepared with toluene diisocyanate [24]. Aliphatic isocyanates are employed in the field of coatings and thermoplastic films, which are utilized for weatherable applications. The estimated yearly growth rate for MDI is 5.2%, while for TDI is 4.6%, and for aliphatic isocyanate is 4.0% [2]. The aromatic diisocyanate is more reactive than the aliphatic one [16]. Two physical-chemical processes—phase separation between hard and soft segments and hydrogen bonding between carbamate bonds—are primarily responsible for the wide range of mechanical properties. Furthermore, the difference in the characteristics can also be attributed to the strong reactivity of isocyanate, even in viscous conditions or at low temperatures [24][17].

There are many mesomeric structures for the isocyanate (-NCO) groups, which can be expressed as follows: -N(δ-)=C(δ+)=O(δ-). The isocyanate group reaction, in which groups are electron donors and acceptors, is made possible by this configuration [56]. The polarization caused by the high electronegativities of the nitrogen and oxygen atoms, which delocalize the electron density toward the nitrogen and oxygen atoms, is the basis for the isocyanate group reactivity, demonstrated in **Figure 2** [17].

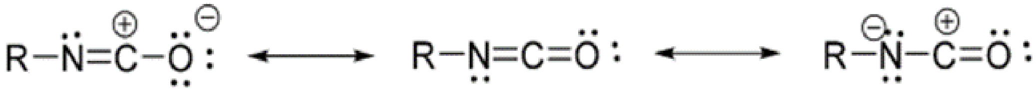

Figure 2. Resonance structures of the isocyanate group. Reproduced with permission [17]. Copyright 2012, American Chemical Society.

Understanding the chemistry of isocyanate is complicated because it involves not only self-addition and trans-condensations but also a range of reactions with other basic substances including amines and alcohols. Additions of alcohol, thiol, or amine are the most significant interactions involving isocyanate. The isocyanate group combines with a hydroxyl group to formulate urethane (**Figure 3a**). Isocyanate creates thio-urethane (**Figure 3b**) and urea bonds (**Figure 3c**) by reacting with thiol and amine, respectively. After reacting with water, volatile carbamic acid is produced, which then breaks down into primary amine and gaseous carbon dioxide (**Figure 3d**) [17].

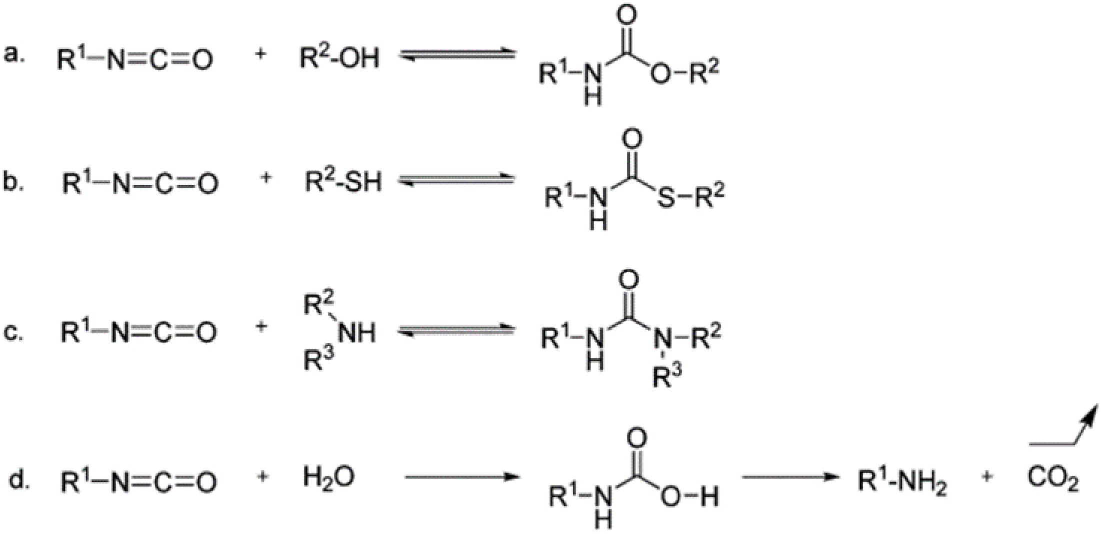

Figure 3. Common reactions used in polyurethane chemistry. Reproduced with permission [17]. Copyright 2012, American Chemical Society.

The hydrogen atom is then moved to nitrogen after the nucleophilic center of XH, where X=O, S, NH, is first joined to the electrophilic carbon of the isocyanate group (**Figure 4**) [17].

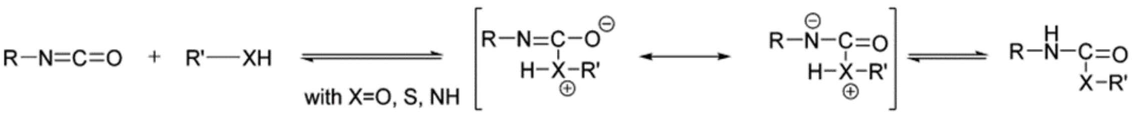

Figure 4. General mechanism of isocyanate/nucleophile reaction. Reproduced with permission [17]. Copyright 2012, American Chemical Society.

1.10. Flame Retardant

Polyurethane foams have a high fire velocity and are particularly easy to ignite. This is because of the polymer matrix's high oxygen, carbon, and hydrogen content as well as its high surface-to-mass ratio, high air permeability, and low aromaticity. Its use is restricted in severe fire scenarios due to its rapid flame growth, which also increases the risk of a fire. Therefore, applying an appropriate flame retardant (FR) to protect the polymer is essential to meet fire test criteria [57–68].

Commonly employed FRs are halogen-containing substances that significantly enhance foam fire behavior. However, non-halogenated substitutes have been more popular than conventional halogenated flame-retardant polymers in engineering plastic during the past ten to fifteen years. The creation of hazardous and dense smoke by halogenated FRs, which harm both the environment and human health, has led to the development of halogen-free flame retardants [58,69,70].

Chemical modification of the ignition process may induce flame retardancy in both the gaseous and condensed phases. In the gas phase, adding FR additives, which release certain radicals, can stop the free-radical mechanism of the burning process. The highly reactive species H• and OH• are then interacted with by these radicals to generate less reactive molecules. Because of this modification to the combustion reaction, the exothermicity of the reaction decreases considerably, which lowers the temperature and, consequently, produces a smaller amount of fuel. The flame retardants can undergo two different kinds of chemical reactions in the condensed phase. At first, the flame retardants may speed up the polymer chain's breakage. In this situation, the polymer drops and slides out of the flame action zone. Secondly, the FR may result in the development of a carbonized layer by chemically altering the breaking polymer chains, at the polymer's surface, which serves as a physical insulator. Such a protective barrier of char restricts the flow of materials, including oxygen and flammable volatile gases. Consequently, there has been a notable reduction in the quantity of breakdown gases generated. Furthermore, it is possible to physically separate the fuel gases from the oxygen, preventing the combustion process from continuing [71].

There are two kinds of flame retardants: additive flame retardants and reactive flame retardants. Additive flame retardants are typically added during the transformation process; they only react with the polymer at higher temperatures when the fire begins. In general, they are hybrids, mineral fillers, or organic compounds, which may contain macromolecules. Reactive flame retardants, on the other hand, are often added to the polymer as monomers or during the post-reaction phase. These fire retardants take part in the chains of polymers [71].

1.11. The Objective of this Research

The primary objective of this project is to assess the impact of recycled canola oil, utilized in the synthesis of polyol, on the properties of RPUFs, compared with those RPUFs derived from new canola oil polyol. The utilization of used canola oil serves a dual purpose in mitigating environmental issues, by shifting away from reliance on petroleum-based materials and by repurposing waste oil, thus preventing its improper disposal and transforming it into a valuable raw material for sustainable production processes. The polyol was derived through a process involving epoxidation and ring-opening, confirmed through multiple characteristic tests including FT-IR, GPC, viscosity, iodine value, hydroxyl value, and many other analyses. Throughout the foam formation process, different flame retardants such as dimethyl methyl phosphonate (DMMP) and expandable graphite (EG) were incorporated to enhance the fire resistance of the RPUFs. Comprehensive investigations were conducted into the mechanical, thermal, and morphological properties, alongside the fire performance of the RPUFs, to clarify the effects of the recycled canola oil polyol on their overall behavior and potential as sustainable materials.

CHAPTER II

MATERIALS AND METHODS

2.1. Materials

Canola oil was purchased from the local Walmart in Pittsburg, KS, USA to obtain the recycled oil by frying food into the oil three to four times to synthesize the polyol. Jeffol SG-522 (sucrose-based polyol with OH# 522) and rubinate M isocyanate (methylene diphenyl diisocyanate-MDI) were gifted from Huntsman in the Woodlands, TX, USA. The chemicals used in the preparation of polyol such as glacial acetic acid, Amberlite ion exchange resin, toluene, hydrogen peroxide, Lewatit MP64 resin, sodium chloride, sodium sulfate, tetrafluoro boric acid (TFA), and methanol were bought from Fisher Scientific in Allentown, PA, USA. For the formulation of RPUFs, the catalysts namely 1,4-Diazabicyclo [2.2.2] octane (DABCO)® T-12 (dibutyltin dilaurate-DBTDL) received from Air Products in Allentown, PA, USA, and JEFFCAT® ZF-22 is a bis-(2-dimethylaminoethyl) ether was supplied by Huntsman. TEGOSTAB B-8404, a silicon surfactant, was obtained from Evonik in Parsippany, NJ, USA. Distilled water, which played a vital role in the formation of RPUFs as a blowing agent, was purchased from the local Walmart located in Pittsburg, KS, USA. Flame retardants like DMMP and EG were obtained from Sigma-Aldrich in St. Louis, MO, USA.

2.1.1. Canola Oil

A rapeseed type known as canola was created by cross breeding the species Brassica rapa and Brassica napus. Currently, canola oil is one of the most widely produced vegetable oils, that are edible, across the globe. The term "canola" denotes a particular cultivar of rapeseed having a minimum percentage (2%) of erucic acid content, along with relatively low glucosinolates and anti-nutritional constituents. Mono- and polyunsaturated fatty acids are also present in large concentrations in it [72,73]. The -OH functional group was introduced by using such unsaturated sites via the epoxidation process, followed by the ring-opening reaction by employing methanol. The structure of the canola oil is illustrated in **Figure 5**.

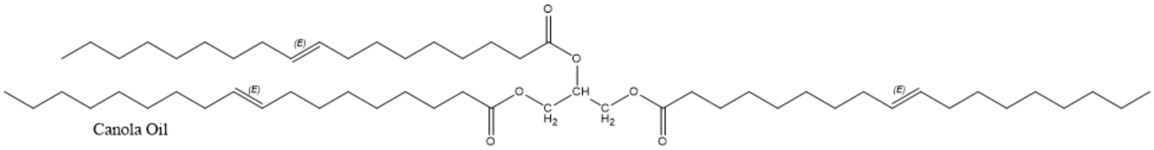

Figure 5. Structure of canola oil.

2.1.2. Methylene Diphenyl Diisocyanate

MDI is manufactured using aniline and formaldehyde as feedstocks [2]. In this examination, MDI was used to synthesize rigid PU foam using biobased polyol. The chemical structure of MDI is given in **Figure 6**.

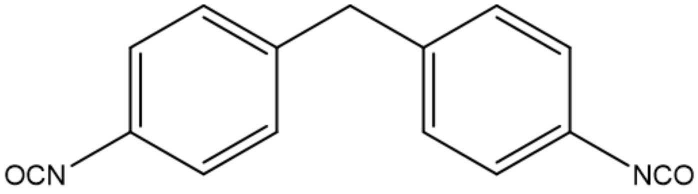

Figure 6. Structure of methylene diphenyl diisocyanate.

2.1.3. Catalyst

Catalysts are vital to industries because they enhance the rate of reaction and offer effective curing processes. It falls into two primary categories: tertiary amine and organometallic-based catalysts, which are commonly utilized. NIAX-A1 and T-12 were used for that, respectively. **Figures 7** and **8** illustrate the structure of NIAX-A1 and T-12, respectively.

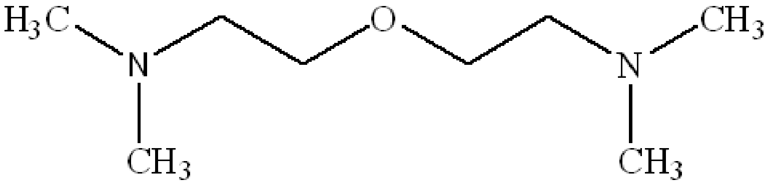

Figure 7. Structure of bis-(2-dimethylaminoethyl) ether (NIAX-A1).

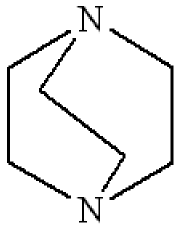

Figure 8. Structure of 1,4-diazabicyclo [2.2.2] octane (DABCO T-12).

2.1.4. Blowing Agent

In this work, distilled water was selected as the blowing agent because of its efficiency, cost-effectiveness, and environmentally friendly properties. Regulating the cellular structure of PU as well as controlling the density was the major purpose of the water. Apart from this purpose, water reacts with isocyanate resulting in the formation of an unstable carbamic acid. It is soon broken down into a primary amine and CO_2, which is the gas responsible for creating the foamed and porous structure.

2.1.5. Surfactant

Strong reactivity exists between isocyanates and hydroxyl groups; nevertheless, the absence of attractive intermolecular contact causes them to form a heterogeneous phase. To mitigate this, stable dispersions are produced by using a surfactant, producing uniform pore size in the foam. Additionally, surfactants prevent bubbles from clumping together during the foaming process, which forms the porous structure of rigid foams. B-8404 surfactant was used in this research for these uses.

2.1.6. Flame-Retardant

The two flame-retardants, DMMP and EG, were used in this study.

2.1.6.1. Dimethyl Methyl Phosphonate

Dimethyl methyl phosphonate is a widely known and effective flame retardant, especially because it is halogen-free [74]. It is a member of the group of flame retardants that contain phosphorus. Because of its specific features, such as a high phosphorus concentration, low viscosity, good solubility, and non-corrosiveness, it is more appropriate for applications in polymer materials [75]. Phosphorus-containing FRs can minimize combustible gases in the condensed phase by developing a char layer [76]. When it comes to controlling fires, DMMP is reported to be 4–6 times more efficient than bromine, a typical halogen fire suppressor [77]. Since DMMP is a liquid FR, it is not sensible to add more DMMP resulting in it moving to the foam's surface, losing the FR, and decreasing the foam's ability to withstand flames. It is also unsuitable to increase the volume of DMMP to achieve enough flame retardancy due to its high cost [74]. **Figure 9** displays the chemical structure of DMMP.

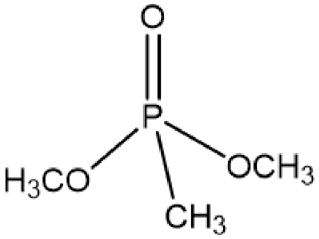

Figure 9. Structure of dimethyl methyl phosphonate.

2.1.6.2. Expandable Graphite

EG is a kind of graphite intercalation compound that originates from natural graphite by chemical processing [78]. It does not consist of halogens [79] and possesses a graphite structure resembling flakes, into which nitric and sulfuric acids are incorporated [76]. EG is more beneficial as a functional carbon material that can be used in a variety of applications, including airtight and military materials, high-power batteries, electrodes, etc., because of its superior characteristics such as low cost, high degree of porosity, improved mechanical properties of the polymers, and many others. Additionally, EG has good flame retardancy in various kinds of polymers, including coatings, PU foams, polyolefins, and many others [78]. As an example, EG, a type of additive that is physically distributed throughout the RPUF matrix, functions best in the condensed phase and can significantly increase the capability of RPUF for flame retardancy [76].

2.2. Synthesis of Canola Oil-Based Polyol

2.2.1. Epoxidation of Canola Oil

The epoxidation procedure was carried out to convert double bonds into epoxy groups in the oil by reacting peroxy acid with it [80]. Before beginning the epoxidation process, the used canola oil (UCO) was filtered using a cone filter with a fine nylon mesh to purify and eliminate contaminants. In the three-necked round-bottom flask (2 liter), 500 g of UCO, 250 ml of toluene, and 125 g of amberlite ion exchange resin were added and mechanically stirred for 15 minutes at room temperature in a water bath. Glacial acetic acid (70.65 g) was introduced dropwise and stirred for 30 minutes after cooling down the reaction mixture to 5-8°C in an ice bath, followed by the addition of around 400 g of 30% hydrogen peroxide. After adding H_2O_2, the temperature was increased to around 70°C and the reaction mixture was stirred for 7 hours with an attached condenser. After the completion of the reaction, the mixture was cooled to room temperature and filtered to remove the unreacted resin. The filtered mixture was washed 7-10 times with a 10% brine solution using a separating funnel. Approximately, 4-5 g of sodium sulfate was added into the mixture as a drying agent and filtered into a flask suitable for rotary evaporation to remove excess solvent. The final product of this reaction is known as epoxidized used canola oil (EUCO).

2.2.2. Ring Opening of Epoxidized Used Canola Oil

This procedure was performed to incorporate the hydroxyl functional group by converting the epoxy group. Methanol and epoxidized used canola oil (EUCO) were taken in a 7:1 mol ratio. At first, 407.66 g of methanol and 0.83 g of tetrafluoroboric acid were mixed in the three-necked round bottom flask (2 liter) and stirred until the temperature was raised to 65-70°C with combined mechanical stirrer, thermometer, and condenser. After maintaining the temperature to 65-70°C, EUCO was added dropwise with an equipped dropping funnel and condenser using a double connection and stirred for 60 minutes. Lewatit MP64 resin (23.10 g) was introduced after cooling down the reaction system to room temperature and continued stirring for around 45 minutes. The mixture was filtered to remove the resin after performing the pH test to confirm the neutral mixture. To eliminate the excess methanol present in the mixture, rotary evaporation was performed. This final thick product was named as the used canola oil polyol (UCOP). The chemical structure of UCO, EUCO, and UCOP are shown in **Figure 10**.

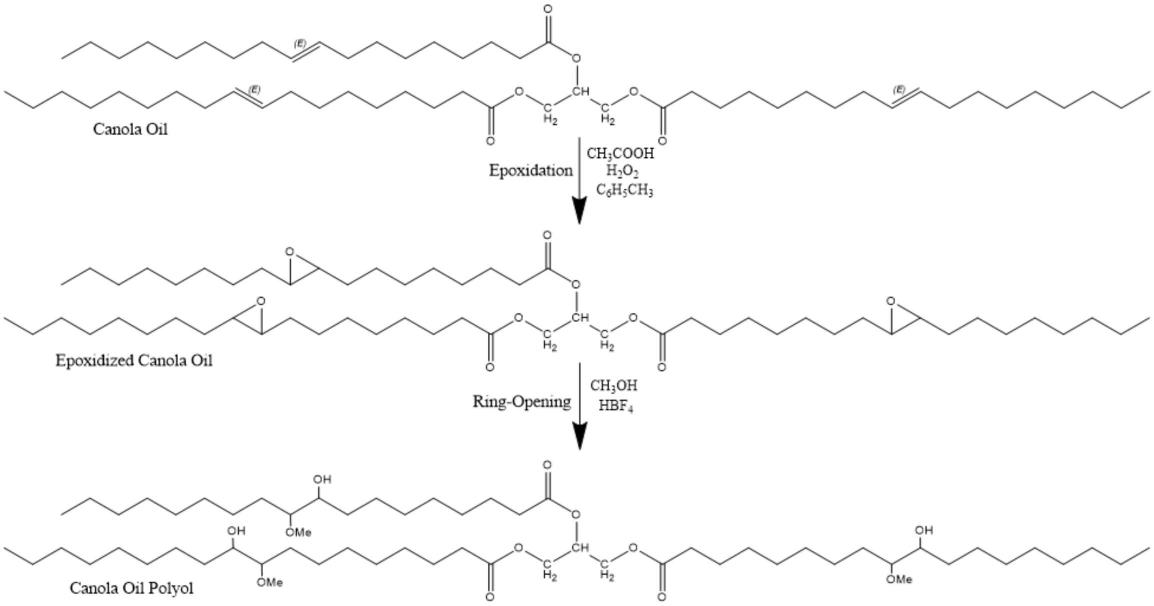

Figure 10. Synthesis of polyol.

2.3. Characterization of Polyol

2.3.1. Iodine Value

The number of unsaturated bonds present in oil and fats is determined by performing iodine value. It is measured as the quantity of iodine in grams that will react with 100 grams of oil [81]. The Hanus method was applied to calculate the iodine value of oil. In a 250 ml Erlenmeyer flask, approximately 0.210 g of oil was dissolved in the 10 ml of chloroform. By using a pipette, 10 ml of Hanus reagent was added to the solution and shaken gently for a few minutes. This mixture was left to sit in a dark room for an hour. Following that, 20 ml of 10% potassium iodide solution and 50 ml of HPLC-grade water were introduced into the mixture and again stirred to obtain a homogeneous solution. Lastly, five to six drops of the starch indicator were added and titrated with 0.1 N sodium thiosulphate ($Na_2S_2O_3$) until the blue color disappeared. The volume of the sodium thiosulphate was noted to calculate the iodine value of the oil.

2.3.2. Epoxy-Oxirane Oxygen Content

The purpose of this titration method is to measure the quantity of epoxy-oxirane oxygen content (EOC%) and to count the number of unsaturated bonds that are converted into the epoxy group using glacial acetic acid and tetraethylammonium bromide (TEAB). At first, 0.250 g of epoxidized oil was transferred into the Erlenmeyer flask and dissolved into the 50 ml of TEAB solution. It was stirred for around 10 minutes to make a uniform solution. This solution was titrated by adding one or two drops of crystal violate indicator, then followed up with 0.1 N perchloric acid. The solution changed from blue to green in coloration. The result of the experiment was recorded to determine the percentage of oxygen content of the samples.

2.3.3. Hydroxyl Value

Hydroxyl value gives information about the number of hydroxyl (OH) groups, which react with isocyanate [82]. The phthalic anhydride pyridine (PAP) method was applied to know how many hydroxyls number were there in polyol according to the American Society for Testing and Materials (ASTM-D 4274). The functionality of polyol is also identified by carrying out this test. In glass bottles, covered via lid, approximately 0.6 g of synthesized polyol was dissolved in 10 ml of OH reagent prepared using phthalic anhydride, imidazole, and pyridine. These bottles were placed into the oven for 70 minutes at 100°C and shaken every 15 minutes. Later, this solution was cooled to room temperature. 10 ml of HPLC-grade water was introduced into the mixture, which was followed by 20 ml of isopropanol and stirred for 10 minutes. After adding a few drops of phenolphthalein indicator, 1 N of sodium hydroxide (NaOH) was utilized for the titration of the mixture. The color was changed from yellow to pink. The volume of the NaOH was noted to calculate the OH number.

2.3.4. Acid Value

The acid value was examined to determine the quantity of acidity in the oil, epoxidized oil, and polyol based on the IUPAC 2.201 standard method with the help of an indicator. Around 3 g of material was added to the 150 ml flask. To dissolve the material, a 30 ml solvent mixture was employed. A phenolphthalein indicator was already present in the solvent mixture with toluene and isopropanol; thus, no additional indicator was required. In the final step, the flak solution was titrated with 0.1 N potassium hydroxide (KOH) until the pink color was stable for at least 10 seconds. The result was recorded and utilized for determining the sample's acid value.

2.3.5. Fourier-Transform Infrared Spectroscopy (FT-IR)

The PerkinElmer Spectrum Two spectrophotometers (**Figure 11**) were utilized for performing FT-IR spectroscopy, providing a quick result for verifying the existence of specific functional groups and covalent bonds in the samples. It displays the spectra in the range of 4000 cm^{-1} to 500 cm^{-1} at room temperature. Spectra are recorded based on transmittance (T%) and wavenumber (v) (cm^{-1}). In this test, infrared radiation is passed through the sample. Some are absorbed via sample while the remains are passed away. Along with displaying the functional group, the FTIR result also reveals any contamination or impurities in the sample.

Figure 11. Fourier-Transform infrared spectroscopy.

2.3.6. Viscosity

The viscosity of the samples was analyzed using an AR 2000 dynamic stress rheometer from TA Instrument, USA (**Figure 12**), with a cone plane diameter of 25 mm and a plate angle of 2°. At a stable temperature of 25 °C, the shear stress rose linearly from 1Pa to 2000 Pa. Information regarding the materials' molecular weight as well as resistance to the flow is provided by viscosity. A substance with a low viscosity also has a low molecular weight; conversely, a high viscosity indicates a larger molecular weight. Thus, viscosity is a key factor in verifying the successful synthesis of the polyol from oil.

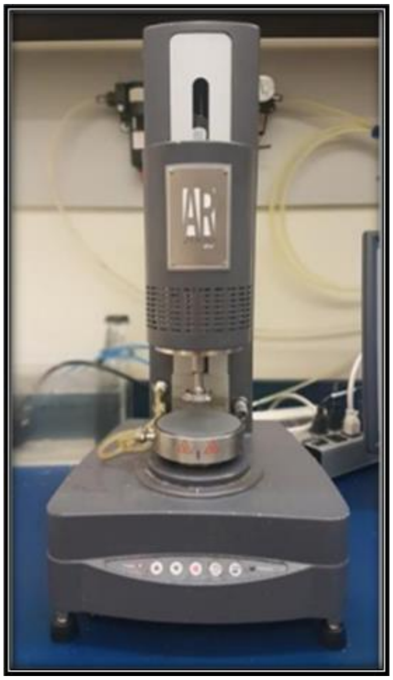

Figure 12. AR 2000 dynamic stress rheometer.

2.3.7. Gel Permeation Chromatography (GPC)

GPC works based on the molecular weight of the substance, which is closely related to that size, by utilizing tetrahydrofuran (THF) as a solvent. This technique is also known as size exclusion chromatography. THF maintains a steady eluent rate of 1 ml/min at 30 °C. The Waters GPC instrument from Milford, MA, USA was used to perform this test, as displayed in **Figure 13**. Four 300 × 7.8 mm Phenogel columns with pore diameters of 50, 102, 103, and 104 Å each have been included in this machine. It separates the molecules according to molecular weight with the help of such different pore sizes. The increment in molecular weight from oil to polyol also illustrated that polyol was successfully produced.

Figure 13. Gel permeation chromatography.

2.4. Preparation of Rigid Polyurethane Foam

The formation of the RPUFs based on new canola oil polyol and used canola oil polyol is displayed in **Table 1**. Utilizing the one-shot free-forming process, bio-based RPUFs were prepared by coupling polyol and isocyanate with the addition of catalyst, blowing agent, surfactant, and flame-retardant. All the components were taken in the same amount in the NCO and UCO-based RPUF formulations; the only difference was in the isocyanate amount according to their hydroxyl number. To obtain RPUFs, synthetic polyol, SG-522, and flame retardants were incorporated in a plastic cup and stirred at a high speed using a mechanical stirrer for a few minutes to create a homogeneous mixture. After adding A-1, water, T-12, and B8404, the mixture was stirred another time. Eventually, the foam rose at room temperature with the addition of isocyanate after being stirred for 5 to 10 seconds using a mechanical stirrer at a high speed. For the curing process, these foams were put at room temperature for around a week before doing any characteristic test. The name of the sample was denoted based on the type of polyol, types of FR, and amount of FR, for example, NCO-DMMP-1 to NCO-DMMP-6, UCO-DMMP-1 to UCO-DMMP-6, NCO-EG-1 to NCO-EG-6 and UCO-EG-1 to UCO-EG-6.

Table 1. NCO and UCO-based RPUF formulation with DMMP and EG. All the numbers are in grams except the wt.% of the DMMP and EG flame retardant.

Ingredient	Control	Sample 1	Sample 2	Sample 3	Sample 4	Sample 5	Sample 6
NCO or UCO-Polyol	10	10	10	10	10	10	10
SG-522	10	10	10	10	10	10	10
A-1	0.18	0.18	0.18	0.18	0.18	0.18	0.18
Water	0.8	0.8	0.8	0.8	0.8	0.8	0.8
T-12	0.04	0.04	0.04	0.04	0.04	0.04	0.04
B8404	0.4	0.4	0.4	0.4	0.4	0.4	0.4
Isocyanate for NCO	30.5	30.5	30.5	30.5	30.5	30.5	30.5
Isocyanate for UCO	29.8	29.8	29.8	29.8	29.8	29.8	29.8
FR	0	1	2	3	4	5	6
% of FR for NCO	0	1.92	3.85	5.77	7.70	9.63	11.55
% of FR for UCO	0	1.95	3.90	5.85	7.80	9.76	11.71

2.5. Characteristics of the Bio-based RPUFs

After curing, the foams were cut into specified shapes and sizes with a table saw to characterize NCO and UCO-based RPUFs. These samples were then utilized to investigate the physical, mechanical, thermal, and morphological properties of RPUFs.

2.5.1. Apparent Density

Density is an essential element that strongly affects the physiomechanical characteristics and performance of the RPUFs, which can modify the structure of foams. It is calculated by taking the mass of the foams and dividing it by their volume. The apparent densities of the foams were examined using the ASTM D1622 standard technique. To measure the density of RPUFs, cylindrical-shaped samples with a diameter of 45 × 30 mm (diameter × height) were employed.

2.5.2. Closed-Cell Content (CCC)

The closed cell content of the foams is measured to determine their thermal insulation properties. Foams are categorized according to their cell structure, which can be either open or closed. To get the results of this test for NCO and UCO-based foams, a sample having a similar shape and size to that used in the density test was selected. The ASTM D2856 method via the use of an Ultrapycnometer, Ultrafoam 1000, as illustrated in **Figure 14**, was used for performing the closed cell content. A chamber and a pressure-temperature sensor are the two major parts of the instrument, which are interconnected within the device. In the first step of the process, the volume of the empty chamber was measured in the presence of nitrogen gas through the valve. Following that, the closed cell content was then identified by inserting a cylindrical sample into the chamber that had known size and volume.

Figure 14. Ultrapycnometer (Ultrafoam 1000).

2.5.3. Compressive Strength

The compressive strength of the foam was used to estimate the maximum force applied to its surface. The ASTM D 1621 technique was executed to measure the compression strength at 10% strain of all the RPUFs by using a Q-Test 2-tensile machine from MST, USA (**Figure 15**), with Blue Hill software. The force was applied parallel to the direction of the foam rise at the strain rate of 3 cm/min from the top of the foam. The cylindrical sample with a 45 mm diameter and 3 mm height was placed at the larger surface area on the compression plate to determine the compression strength of all the RPUFs.

Figure 15. Q-Test 2-tensile machine.

2.5.4. Scanning Electron Microscope (SEM)

The surface images of the specimen were displayed using a scanning electron microscope. To conduct this test, the specimen was initially cut with a sharp blade into a square shape that was about 0.5 cm^3 in size on each side. It was then linked with a conductive carbon tap to prevent any charging effects during imaging. The sample was then placed in a magnetron sputtering unit from Kurt J. Lesker Company (Jefferson Hills, PA, USA, **Figure 16(a)**) to coat its surface with an extremely thin layer of gold (Au) to improve the quality of the images. Argon gas was used to flush the system multiple times. In addition, the samples were exposed to the plasma beam for forty seconds under a 50-mBar vacuum. A Thermo Scientific Phenom Pure desktop SEM from the Sioux company in the Netherlands, shown in **Figure 16 (b)**, was used to take the photos after the sample had been coated with gold.

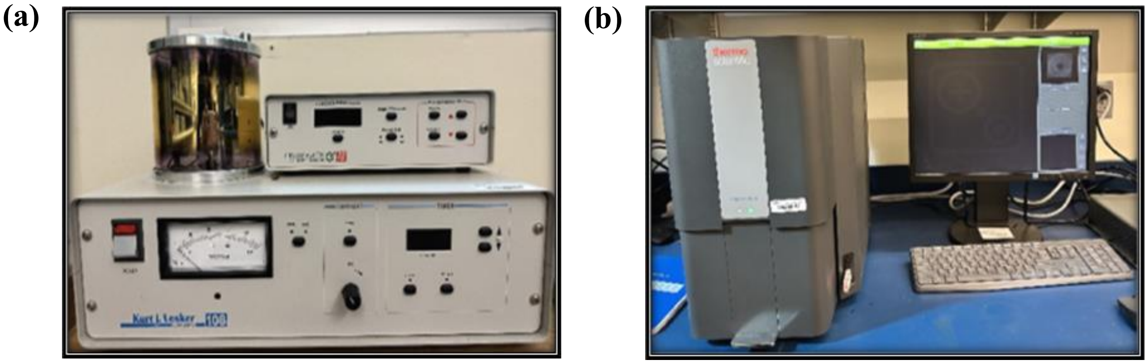

Figure 16. (a) Gold layer deposition unit **(b)** Thermo Scientific Phenom SEM unit.

2.5.5. Horizontal Burning Test

To investigate the fire performance of DMMP and EG on RPUFs, a horizontal burning test was performed utilizing the ASTM D 4986-18 standard test procedure. A rectangular sample of 150 × 50 × 12.5 mm^3 in length, width, and thickness, respectively, was inserted horizontally into the instrument after recording its weight. After providing fire directly for 10 seconds, the self-extinguished time and the weight of the sample were noted to calculate the percentage of weight loss, after burning the sample. This test was conducted in a fume hood with high ventilation to remove fumes released during decomposition, as displayed in **Figure 17**.

Figure 17. Horizontal burning test setup.

2.5.6. Thermogravimetric Analysis (TGA)

Thermogravimetric analysis, an analytical technique that involves applying continuous heat and recording the material's weight loss as a function of temperature, was used to gather information regarding the substance's thermal stability. The TA instrument (TGA Q500, New Castle, DE, USA), as seen in **Figure 18**, was utilized to understand the thermal behavior and decomposition of the DMMP and EG-containing RPUFs. It was performed under the nitrogen flow from room temperature to 600°C at a ramp rate of 10°C/min.

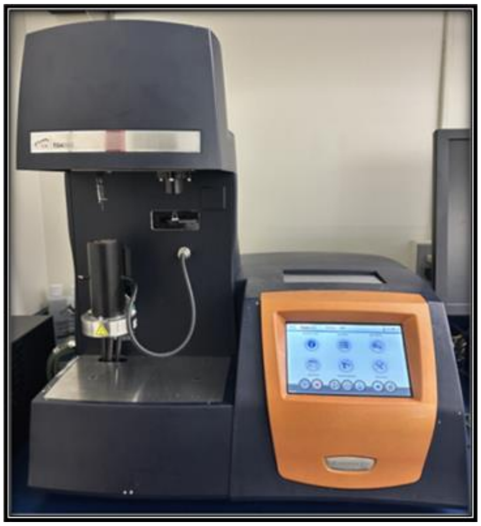

Figure 18. Thermogravimetric analyzer.

CHAPTER III

RESULTS AND DISCUSSIONS

The replacement of petroleum-based polyols with bio-based polyols using pure and used oils in the production of RPUFs marks a significant shift towards environmentally friendly materials. Various experiments were carried out to confirm the successful synthesis of the bio-based polyol and to investigate the physicomechanical and thermal stability of the resulting rigid PU foams.

3.1. Properties of Oils, Epoxides and Polyols

3.1.1. Iodine Value

The iodine value was measured using the Hanus method to determine the quantity of unsaturation or double bonds present in oils and epoxides oils. Used canola oil had an iodine value of 106.71 g I_2/100 g, which is slightly less than the iodine value of pure canola oil, which was 119.56 g I_2/100 g. Based on this data, stoichiometric calculations were performed to determine the quantity of reagents required for the epoxidation process. After the epoxidation procedure, this value dropped for EUCO by 2.28 g I_2/100 g and for ENCO by 1.19 g I_2/100 g. This downward trend demonstrates that the epoxidation process was successful in converting double bonds into the epoxy group.

3.1.2. Epoxy-Oxirane Oxygen Content

The percentage of epoxide groups in a sample is determined by the presence of oxirane number in it. This epoxide number was 5.95% in the EUCO after the UCO underwent epoxidation with hydrogen peroxide and acetic acid in the presence of the catalyst. This result was 6.61% for ENCO. The epoxy proportion in the UCO polyol was found to be approximately 0.12%, while it was around 0.21% in the NCO polyol, after the ring-opening process. This indicates that hydroxyl groups had replaced the epoxide ring.

3.1.3. Hydroxyl Value

This experiment was conducted to determine how many OH functional groups are present in a substance. The hydroxyl number, that determines the reactivity and quantity of isocyanate necessary for the synthesis of PUs, is one of the most significant characteristics of polyols. The hydroxyl number of the NCO polyol in this investigation was 244.43 mg KOH/g, whereas the UCO polyol showed a little reduction in OH number, measuring about 214.03 mg KOH/g. The amount of MDI essential to create the RPUFs was calculated by utilizing this number.

3.1.4. Acid Value

To produce the PU foams made from waste and pure canola oil, an amine-based catalyst was utilized. Foaming may be controlled by an extremely high acid value of the polyol since the acidic polyol and amine-based catalysts may not react as predicted. The acid value of the UCO polyol was 1.16 mg KOH/g, whereas UCO and EUCO had an acid value of 0.80 and 1.05 mg KOH/g, respectively. Similarly, 0.62, 0.86, and 1.35 mg KOH/g acid values were observed for NCO, ENCO, and NCOP, respectively. This low value has minimal effect on the catalysis that produces PU foam. The reaction of PUs is catalyzed by ternary amines; for that, a low acid value indicates a higher level of reactivity during the foaming process and suitable catalytic activity without side reactions that neutralize acids and bases [83].

3.1.5. Viscosity

The term viscosity refers to the study of a material's resistance to flow. The hydroxyl number and molecular weight of the sample have an impact on viscosity. The substances' increasing viscosity is correlated with their rising molecular weight and hydroxyl number [84]. The viscosity of the NCO was found to be 0.030 Pa.s., whereas the UCO's viscosity was measured to 0.023 Pa.s. For the EUCO and UCOP, the obtained viscosity was 0.072 Pa.s and 1.198 Pa.s, respectively. 0.093 Pa.s and 0.750 Pa.s were the recorded viscosity for the ENCO and NCOP, respectively. The polyols' lower viscosity facilitates more easily processed materials and uniform mixing [83]. The higher viscosity from oil to polyol indicates a rise in molecular weight.

3.1.6. Fourier-Transform Infrared Spectroscopy

Fourier spectroscopy is one of the simplest methods to confirm the synthesis of the polyol and epoxidized oil from NCO and UCO, which represents the chemical bonds present in the substance. The FT-IR spectra of different vegetable oils usually show =C-H stretching vibration in the range between 2989 cm^{-1} to 3029 cm^{-1} [85]. This peak appeared at around 3007 cm^{-1} in NCO and UCO, indicating the presence of the unsaturated double bond in the oil [86]. This peak vanished after the epoxidation procedure, and a new peak emerged at about 825 cm^{-1}, which was linked to the epoxy (C-O-C) group [87] in the epoxidized used canola oil. In ENCO, this peak was seen at approximately 823 cm^{-1}. The specific absorption bands of polyols are seen between 3300 and 3450 cm^{-1}, which correspond to the stretching vibration of O–H [88]. This peak was developed at around 3457 cm^{-1} and 3454 cm^{-1} in UCO polyol and NCO polyol, respectively. These infrared spectra are depicted in **Figure 19 (a)** and **(b)**, which emphasize the characteristic peaks in this substance that demonstrate the successful synthesis of polyol, which is useful in the synthesis of RPUFs.

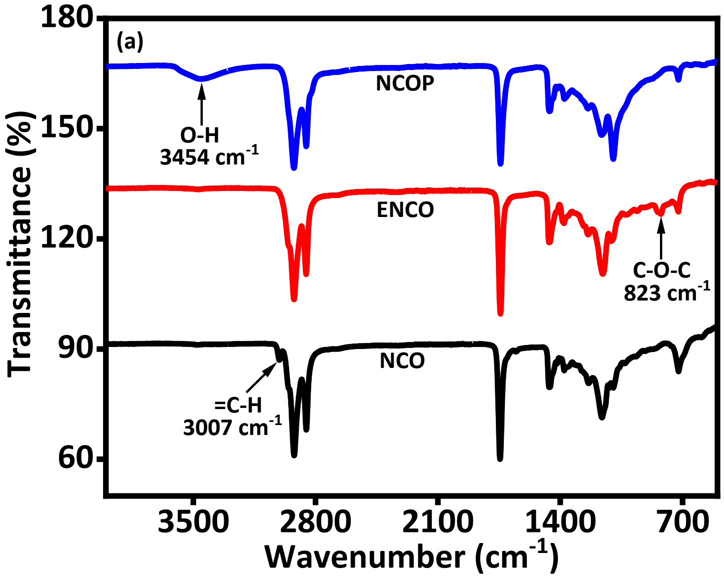

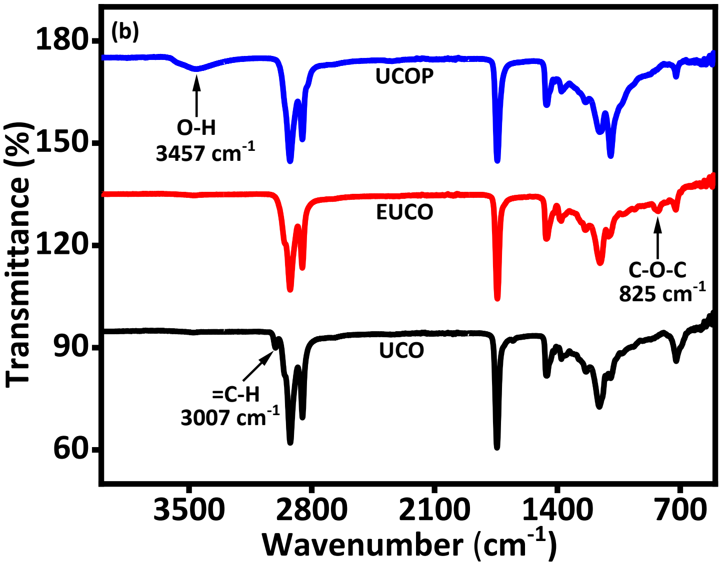

Figure 19. FT-IR spectra of **(a)** NCO, ENCO, and NCOP; and **(b)** UCO, EUCO, and UCOP.

3.1.7. Gel Permeation Chromatography

This technique is an analytical approach utilized for tracking reaction advancement. By utilizing a particular GPC column with varying weight ranges, substances can be distinguished. The presence of porous beads within the column facilitates the entry of smaller molecules into the pores, leading to longer retention times. Conversely, larger molecules encounter fewer pores, resulting in shorter retention times and easier elution. Because of that the UCO-polyol came out first with a retention time of 32.02 minutes, while EUCO and UCO had a higher retention time, which was 32.27 and 32.13 minutes, respectively. This time was 32.11, 32.27, and 32.04 minutes for NCO, ENCO and NCOP, respectively. The GPC chromatogram for both the oils, epoxidized oil, and polyols is ascribed in **Figure 20 (a)** and **(b)**.

The decrease in polyol retention time reveals a rise in the molecular weight of polyol. The polyol's small addition peak at around 30.40 minutes suggests that side reactions corresponding to oligomerization took place during the ring-opening reaction. The reaction between the freshly generated hydroxyl and the preexisting epoxy groups resulted in oligomerization [29]. This peak is also associated with dimers and trimers and is linked to oligomerization and changes in the fatty acid substituent [89]. A longer retention period for EUCO and ENCO may arise due to the polar-polar interaction between the polar nature of epoxidized oil and the polar silica gel found in the GPC column.

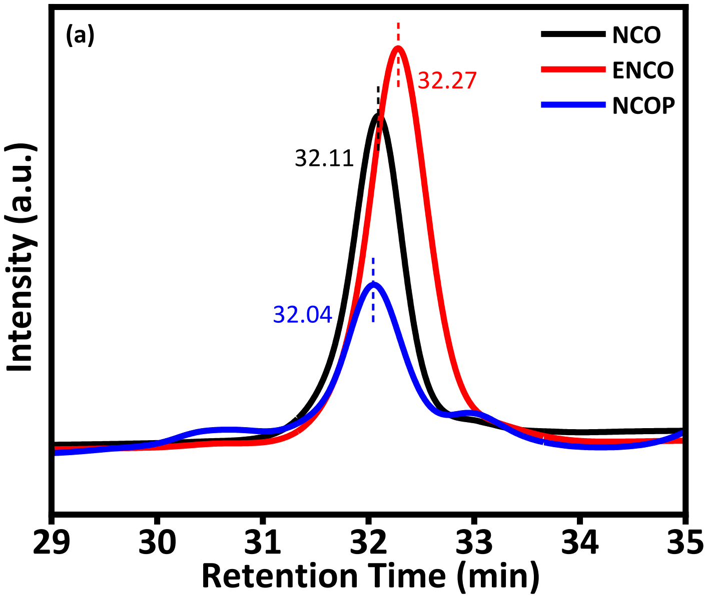

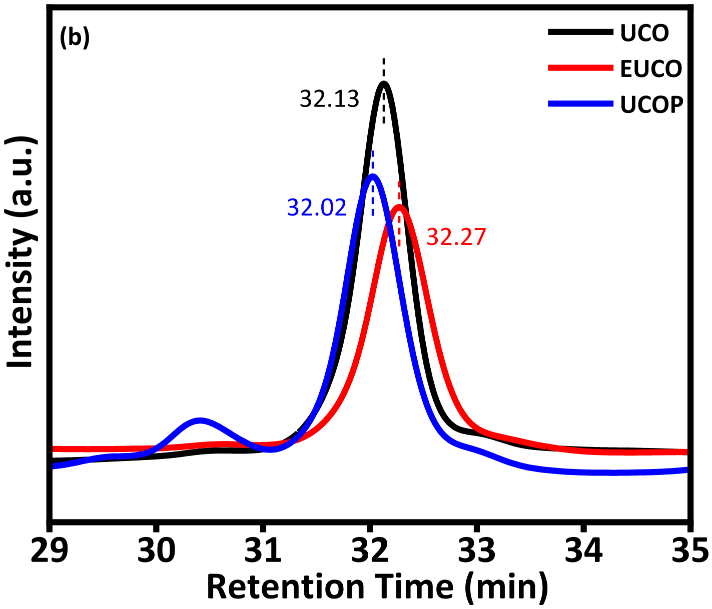

Figure 20. GPC curves of **(a)** NCO, ENCO, and NCOP; and **(b)** UCO, EUCO, and UCOP.

3.2. Properties of the Rigid Polyurethane Foams

Once the suitable properties of polyol were identified, RPUFs with varying amounts of flame retardants were developed. To analyze the properties of the RPUFs, several tests were performed, which illustrate the influences of UCO compared with NCO on RPUFs. Physicomechanical properties typically encompass parameters such as density, compressive strength, and many others. Thermal stability assessment involves examining the foam's behavior under different temperature conditions, including its flame retardancy, and thermal conductivity. Initially, the foams were cut into standardized sizes by using a table saw to characterize NCO and UCO-based RPUFs. The samples, which were gained by cutting the foams, were then used to investigate not only the physical, mechanical, and thermal properties but also utilized for determining the morphology of the foams.

3.2.1. Apparent Density

A detailed examination of the physical characteristics of biobased rigid PU foams was conducted to determine the effects of UCO and NCO-based polyol and flame retardants on the composition of the material on an overall basis. One crucial factor that significantly affects the characteristics and functionality of RPUFs is their density, determining the physical and mechanical properties of RPUFs [90][83]. The effect of polyols and FRs on density defines its functions for numerous purposes such as the foam's strength, modulus, and capacity to absorb energy [91]. Foam density generally gets affected by the degree of foaming, which is influenced by the type and quantity of foaming (blowing) agent [90]. The distilled water, a chemical blowing agent, used in this investigation was taken in a constant quantity. However, the amount of different FRs was varied. Using a specimen with a cylindrical shape, the average apparent density was measured.

The apparent density of RPUFs with EG and DMMP based on UCO and NCO polyol is depicted in **Figures 21 (a)** to **(d)**, and the findings indicate that flame retardants have a major impact on these characteristics. An upward trend was seen in the foams containing EG, with higher concentrations of expandable graphite for both NCO- and UCO-based RPUFs. This might be connected to the rise in polyol viscosity that occurred after EG was added to the RPUF [91]. Because of that the weight of the RPUF rises with the addition of EG, which impacts the degree of foaming [78]. An additional explanation for this is that the acidic groups on the surface of EG mitigate the catalyst's effects and slow down the foams' rising time. As a result, the apparent densities of the foams increased [92]. In comparison to pure RPUFs, which had a density of 38.88 kg/m^3, the density of RPUFs containing EG was greater, ranging from 40.25 kg/m^3 to 52.04 kg/m^3 for UCO-EG-1 to UCO-EG-6. As the amount of EG grew, the density of the NCO-EG RPUFs increased from 35.65 kg/m^3 to 47.78 kg/m^3. Regarding the density of RPUFs with DMMP, the opposite tendency was noted for UCO-based RPUFs. The density of the foams reduced as the DMMP content increased. The value decreased from 34.66 kg/m^3 in UCO-DMMP-1 to 32.70 kg/m^3 in UCO-DMMP-6. A similar trend was also witnessed for the NCO-DMMP-1 to NCO-DMMP-6, which had densities ranging from 32.70 kg/m^3 to 35.61 kg/m^3.

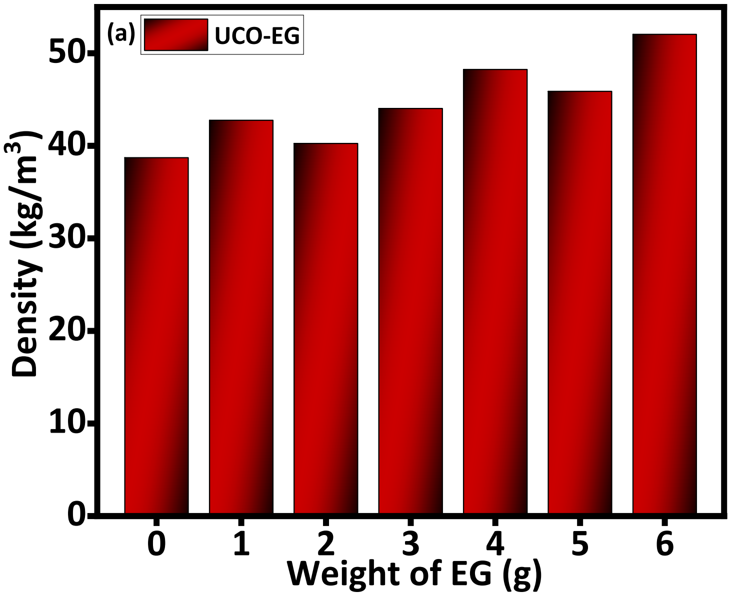

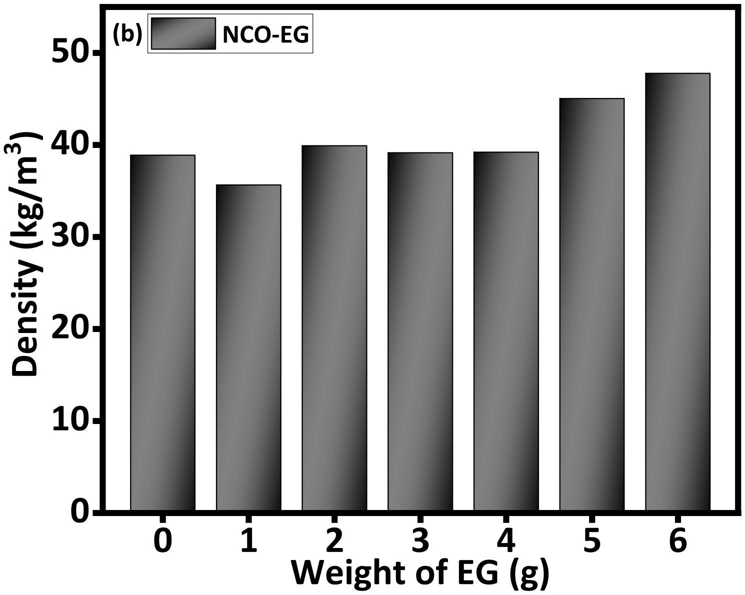
(b)
NCO-EG
Density (kg/m^3)
0
10
20
30
40
50
0
1
2
3
4
5
6
Weight of EG (g)

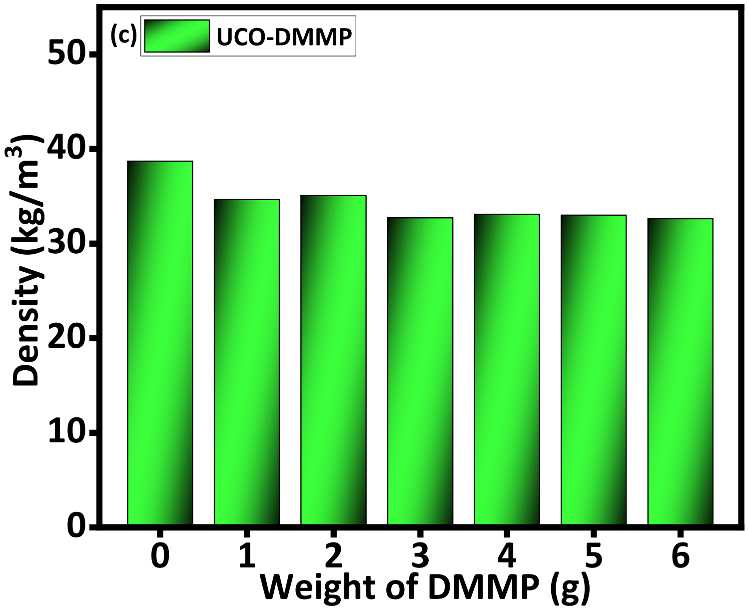
(c)
UCO-DMMP
Density (kg/m^3)
0
10
20
30
40
50
0
1
2
3
4
5
6
Weight of DMMP (g)

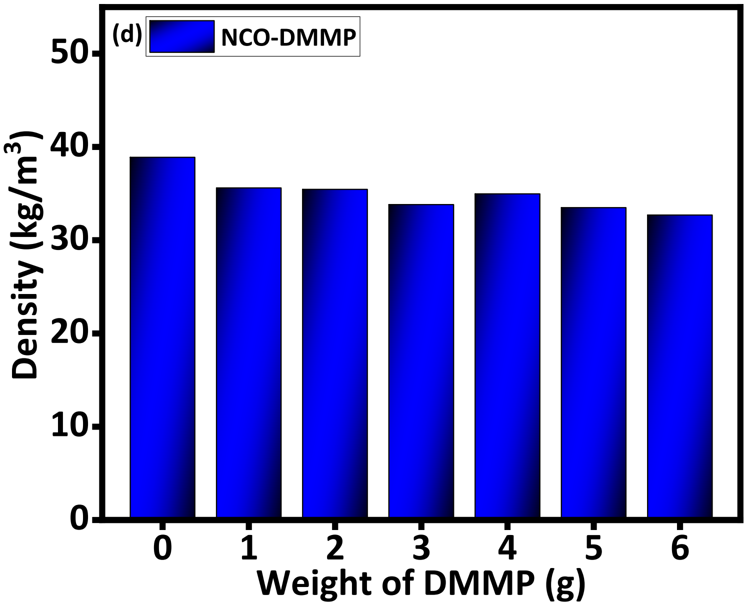

Figure 21. Apparent density of rigid polyurethane foams based on **(a)** UCO-EG **(b)** NCO-EG **(c)** UCO-DMMP, and **(d)** NCO-DMMP with varying amounts of FRs.

3.2.2. Closed-Cell Content

Another method for measuring the properties of synthesized foams is the closed-cell content, which identifies the foams' features related to thermal insulation [93]. One of the demands for improved thermal insulation in rigid PU foams is a high closed-cell content. **Figures 22 (a)** to **(d)** show the measured closed-cell content for the rigid PU foams treated with various flame retardants. Comparing foams with DMMP FR to those without FRs, a slight decrease in the closed-cell content was noticed with the increasing amount of DMMP. With slight fluctuation, this declining trend was measured from 91.88% to 91.13% in UCO-DMMP and from 93.92% to 90.24% in NCO-DMMP. As the amount of EG in the RPUFs increased, there was a small improvement in the closed-cell content observed. This result increased from 92.02% to 92.65% for UCO-EG, whereas it climbed slightly from 91.72% to 92.61% for foams based on NCO-EG, with some variation. The closed-cell content of foam without FRs was 94.84%. However, the average closed-cell content for all four sets of foams was in the range of 90% to 95%, indicating low air transmission in the empty spaces along with superior thermal insulating properties of the foams. These higher closed cells limit airflow within the cellular structure, which inhibits simple access to oxygen during burning as well as inhibiting easy heat transfer from one cell to another. This results in enhanced insulating properties [93].

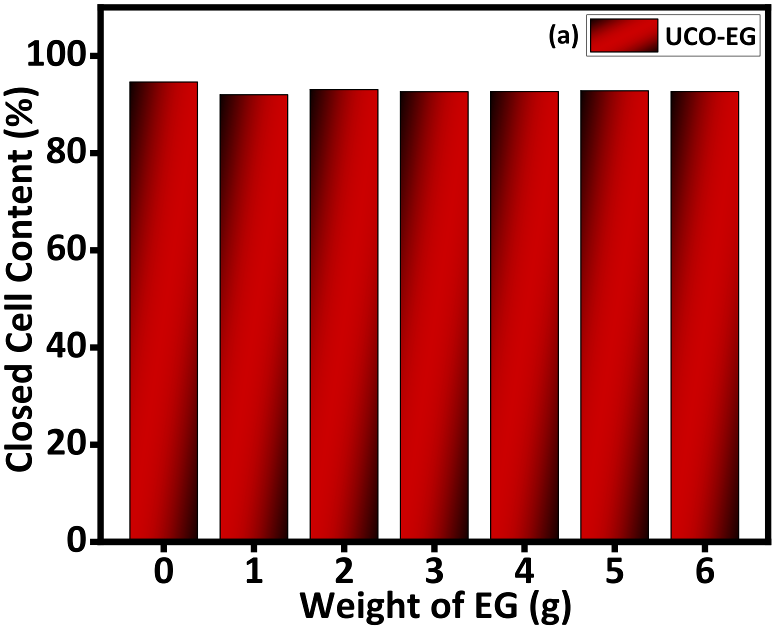

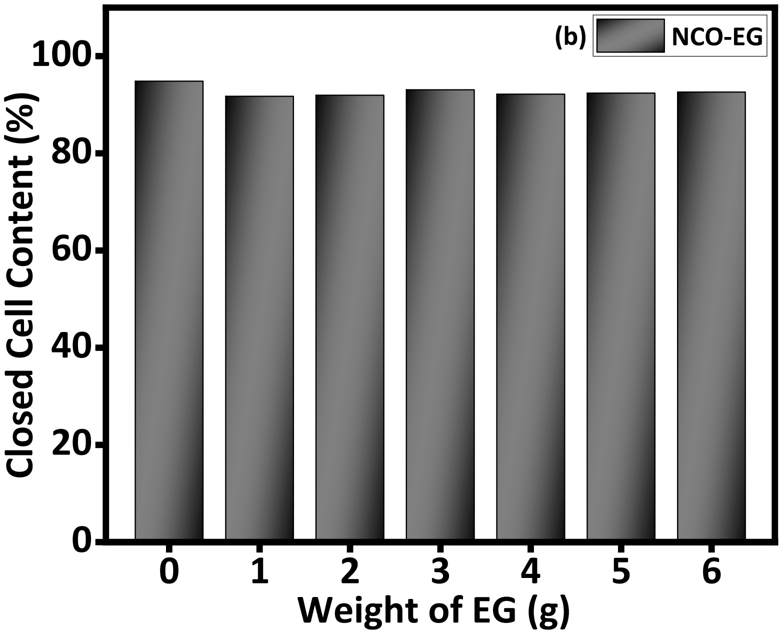
(b)
NCO-EG
Closed Cell Content (%)
0
20
40
60
80
100
0
1
2
3
4
5
6
Weight of EG (g)

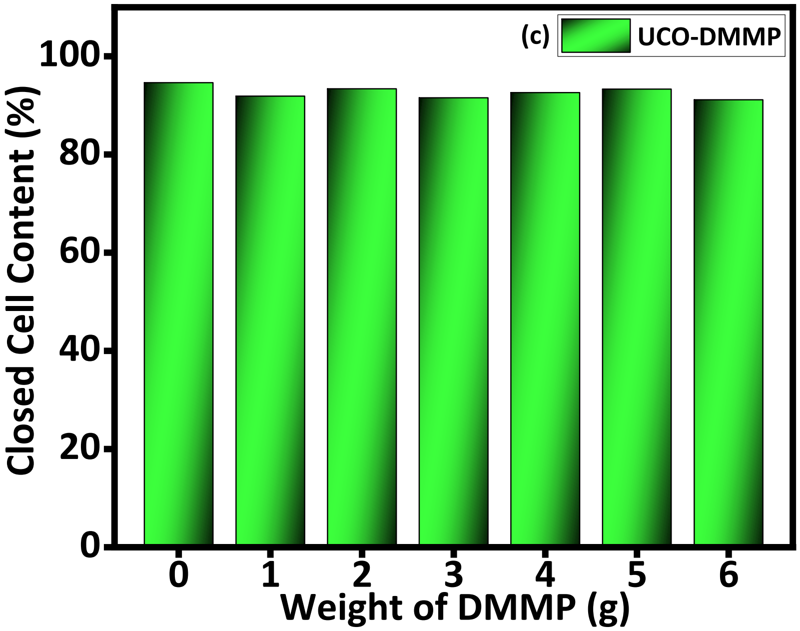
(c)
UCO-DMMP
Closed Cell Content (%)
0
20
40
60
80
100
0
1
2
3
4
5
6
Weight of DMMP (g)

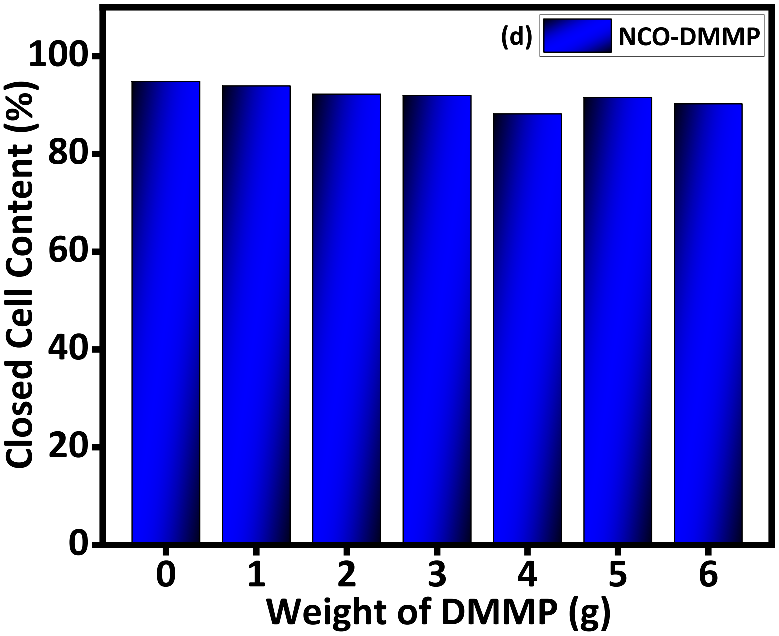

Figure 22. Closed-cell content of rigid polyurethane foams based on **(a)** UCO-EG **(b)** NCO-EG **(c)** UCO-DMMP, and **(d)** NCO-DMMP with varying amounts of FRs.

3.2.3. Compression Strength

One of the most important factors for the various applications of RPUFs is their mechanical properties. To assess the mechanical properties of rigid PU foams, it is crucial to analyze their compressive strength, at which the foams' failer to return to their original forms was evaluated as well as compared in this research to examine the effects of an increasing amount of the different flame retardants. This value was observed after a 10% strain or compression. **Figures 23 (a)** to **(d)** represent the compressive strength of rigid foams, created using NCO and UCO polyol, treated with two distinct flame retardants.

The compression strength of the foam containing EG was higher with the addition of EG in increasing amounts as compared to neat foam. Comparing the foam with EG added in increasing amounts to the foam without, the foam with EG showed a better compression strength. It has increased because of the presence of EG in the RPUFs. In general, the apparent density rose when EG was present. The density of the samples has a significant effect on the compression stress. Compression stress was greater in the foams with higher densities. As a consequence, EG improves the mechanical properties of the foams [94].

Another explanation is that the EG in RPUF might tolerate a heavier load [79]. The compression strength was 250 kPa for the UCO control and 270 kPa for the NCO control. These results were increased by 360 kPa and 320 kPa in UCO-EG-6 and NCO-EG-6, respectively. The slight variability observed in these data could be attributed to the solid EG particles, which might not fully interact with the RPUF matrix. On the contrary, the mechanical characteristics of the RPUFs were adversely affected by DMMP. This value declined with the increasing amount of DMMP, dropping from 230 kPa to 180 kPa in UCO-based RPUFs and from 230 kPa to 190 kPa in NCO-based RPUFs. Nonetheless, this outcome exceeded the minimal value for typical RPUFs of 150 kPa at a density of 30 kg/m^3 [95].

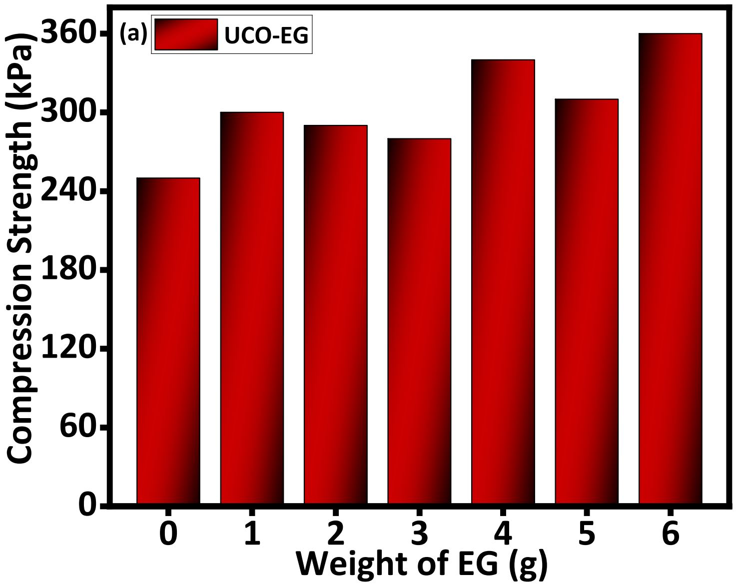
(a)
UCO-EG
Compression Strength (kPa)
0
60
120
180
240
300
360
0
1
2
3
4
5
6
Weight of EG (g)

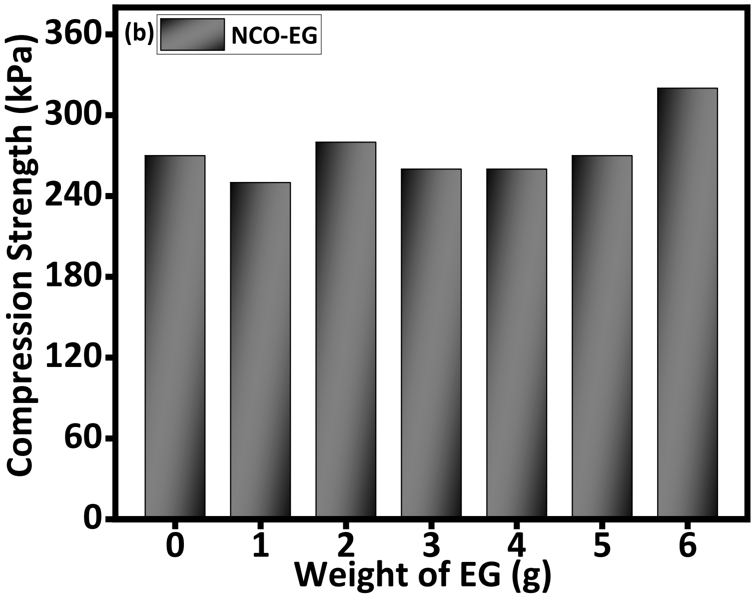
(b)
NCO-EG
Compression Strength (kPa)
0
60
120
180
240
300
360
0
1
2
3
4
5
6
Weight of EG (g)

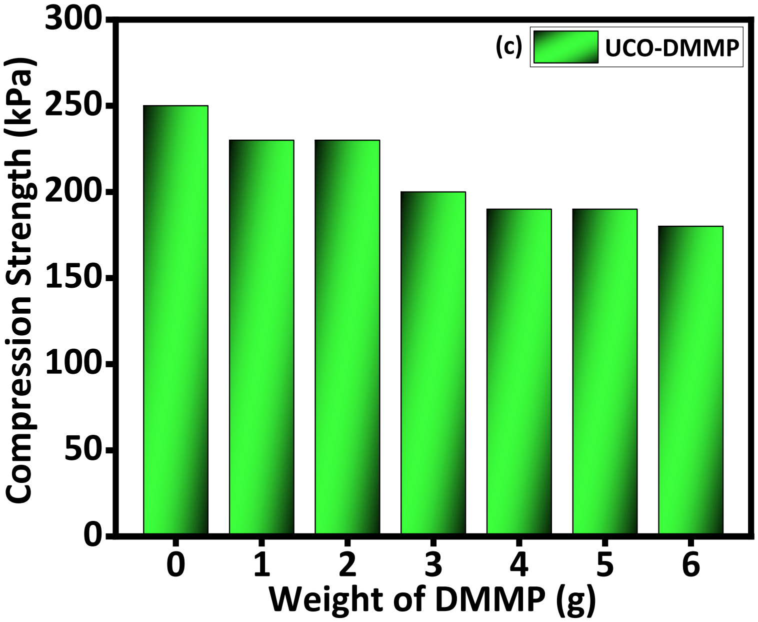

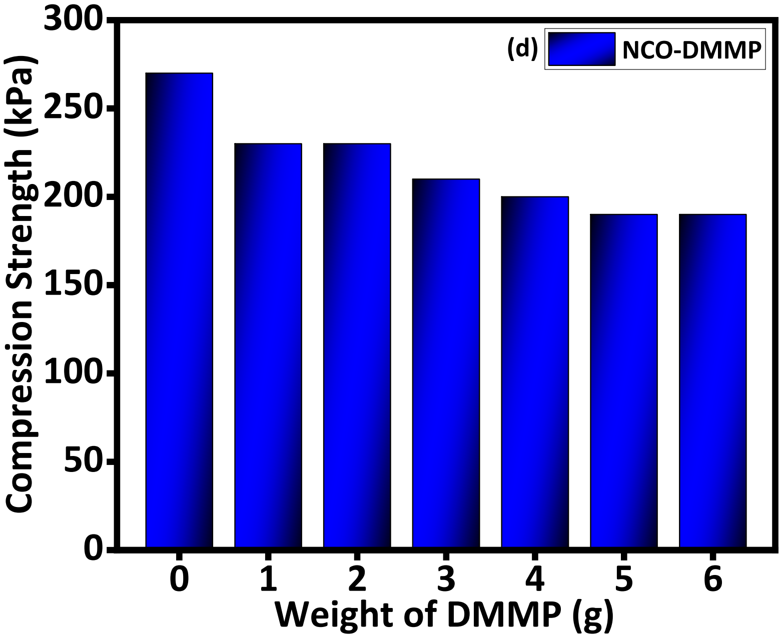

Figure 23. Compression strength of rigid polyurethane foams based on **(a)** UCO-EG **(b)** NCO-EG **(c)** UCO-DMMP, and **(d)** NCO-DMMP with varying amounts of FRs.

3.2.4. Scanning Electron Microscopy

SEM analysis was performed to investigate the cell morphology and structure of RPUFs. The physical characteristics of RPUFs were significantly influenced by their microstructure [79]. **Figures 24** to **27** are the images from the scanning electron microscopy for all the synthesized RPUFs with uniform cellular structures comprising EG and DMMP. The average cell size for the PU foam without any FRs was 170 µm for the UCO-based RPUFs, whereas the NCO-based foams had an average cell size of 167 µm. Adding flame retardant, however, causes the rigid foam cells to alter in size. In foams that included EG, a little decrease in cell size was seen as EG was added in higher quantities, leading to a higher number of cells as well as high compression strength, which is often influenced by the foam's cell structure including cell wall strength, size, and homogeneity [96]. In UCO-based RPUFs, an average cell size drops from 213 µm to 118 µm when the concentration of EG is increased from 1 g to 6 g. In the foams made using NCO, this size decreased from 192 µm to 144 µm. The smaller particles of EG function as a blowing nucleation agent, which increases cell concentration and decreases cell size [97]. These data support the density values. The reaction mixture of PU foam experiences an increase in acidity when the amount of EG grows. This phenomenon causes the foam to rise more slowly and become denser [92]. In the case of DMMP, when DMMP concentration was increased from 1 g to 5 g, there was a gradual rise in cell structure; however, when 6 g of DMMP was added, there was a sharp increase in cell size. The UCO-based foams containing DMMP-1 to DMMP-6 had cell sizes ranging from 160 µm to 247 µm. Foams derived from NCO also show an increase in cell size upon adding additional DMMP. The cells in these foams ranged in size from 187 µm to 232 µm. The reason behind this was the lower density of the foams treated with DMMP. The density influences the size of the cells. Lower density is associated with RPUFs' large cell structure [90]. The average cell size of all the foams is provided in **Table 2**.

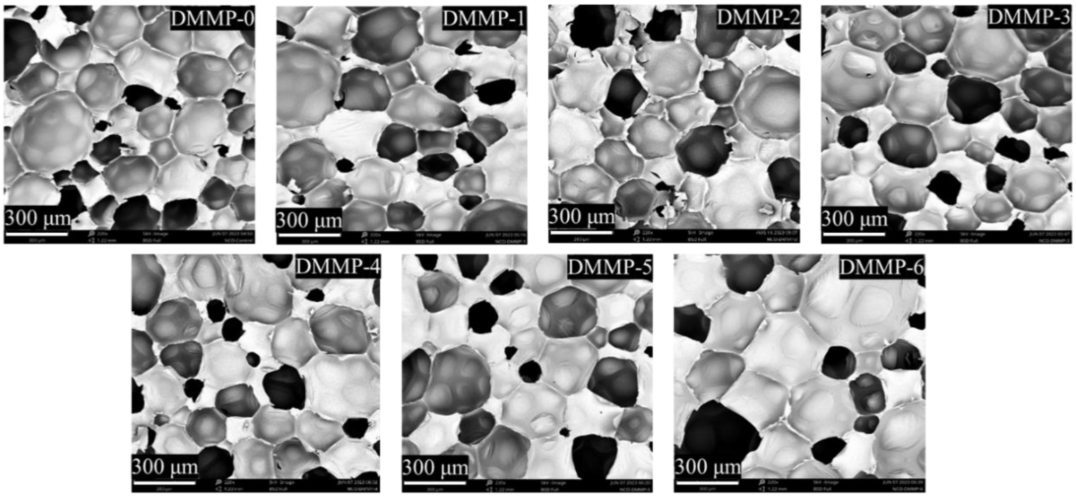

Figure 24. SEM images of NCO-DMMP based RPUFs.

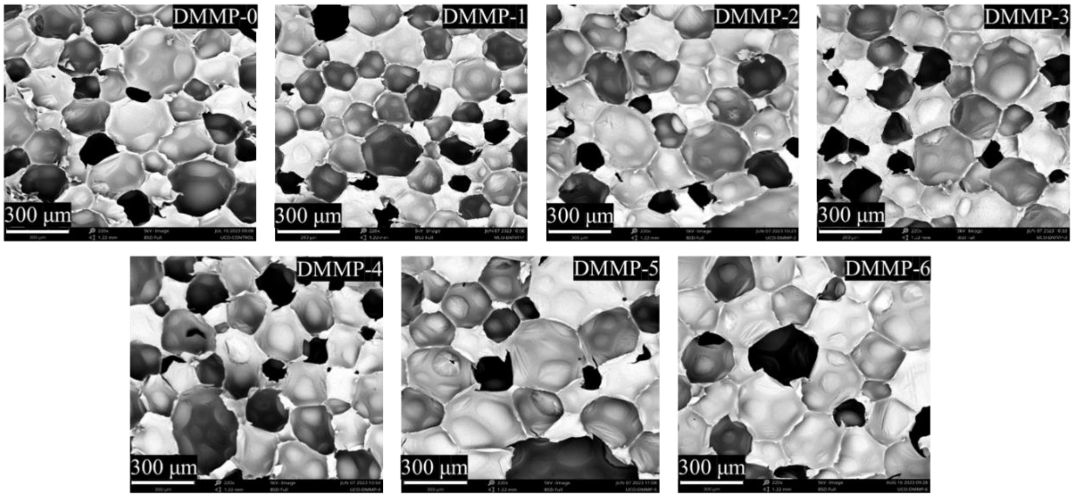

Figure 25. SEM images of UCO-DMMP based RPUFs.

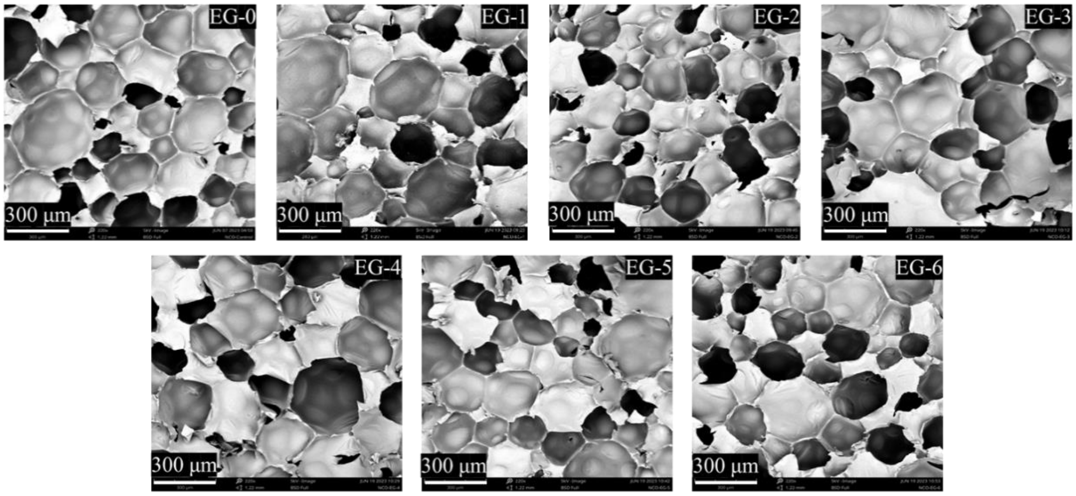

Figure 26. SEM images of NCO-EG based RPUFs.

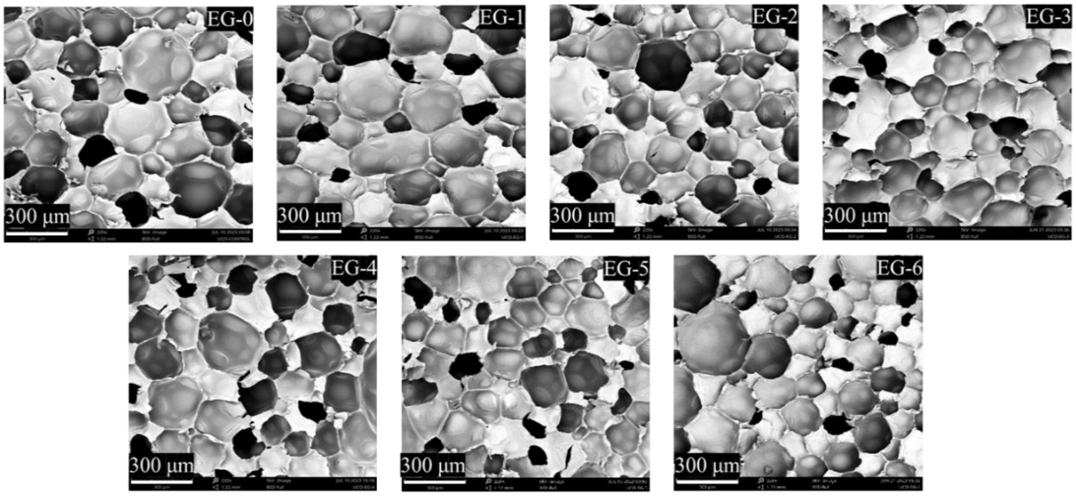

Figure 27. SEM images of UCO-EG based RPUFs.

Table 2. Average Cell size of RPUFs based on UCO and NCO with different amounts of FRs.

Weight of FR (g)	**Cell Size (μm)**			
	UCO-EG	**NCO-EG**	**UCO-DMMP**	**NCO-DMMP**
0	170	167	170	167
1	213	192	160	187
2	170	167	174	202
3	147	163	182	192
4	153	170	182	192
5	139	150	225	196
6	118	144	247	232

3.2.5. Thermogravimetric Analysis

Performing thermogravimetric analysis (TGA) and derivative thermogravimetric analysis (DTGA) helps to explain the thermal transition behavior of rigid PU foams. This test is carried out under a nitrogen atmosphere. TGA and DTGA curves, about their weight loss under the influence of different FR concentrations, are displayed in **Figures 28** to **32**. It was observed that the PU foams without flame retardant showed three main degradation steps (**Figure 28**). The first degradation was associated with the decomposition of the main chain in the PU foams based on UCO [83], at around 297°C. The remaining two degradations corresponded to the pyrolysis of polyol and isocyanate, and the decomposition of char layer [83]. This degradation occurred at the temperature of around

335°C and 446°C, respectively. These decompositions were noticed at approximately 308°C, 342°C, and 456°C, respectively, in the foams prepared from the NCO. The addition of FRs increases the thermal stability of the PU foams. The addition of DMMP into the PU foams depicted an additional degradation step in the temperature range of 138°C to 160°C in the UCO-based foams. This decomposition was attributed to the volatilization and the thermal pyrolysis of the DMMP flame retardant. The boiling point of DMMP is 181°C [98]; for that, the less-stable P-O-C bond of DMMP was easily volatile at around this temperature range [83,99]. As a result, phosphorus-containing components are effectively eliminated into the gas phase by DMMP. Meanwhile, any residual DMMP may still be present in the matrix and hence have a minor flame-retardant impact during the condensed phase, which prevents fire [83,99]. As the DMMP level was raised, the foams' ultimate char content rose, as shown in **Figures 29** and **30**. This implies the formation of stable char, which could act as a barrier to improve flame retardancy. This degradation of DMMP was at approximately 145°C to 165°C in the case of RPUFs prepared using NCO. The other degradations were like the decompositions that occurred in the neat PU foam.

The foams having EG also showed better thermal stability of the RPUFs. However, due to the relatively larger particle size of EG, it exhibits microscopic dispersion heterogeneity in the matrix. As a result, there is some reasonable variation in the residual char yields with a higher concentration of EG [99]. With the decomposition of the hydrocarbon chain in the PU foam based on UCO treated with EG, EG activates and starts to expand, forming a protective char layer on the surface of the foam [92]. This first degradation occurred around 305°C seen in **Figure 31**. The irreversible expansion of the graphene structure results from EG pyrolysis, which is composed of SO_2, CO_2, and water that becomes trapped and escapes close to the graphitic structure's edges [92]. The second degradation was related to the decomposition of polyol and isocyanate of PU foams at around 340°C, as described earlier. The last disintegration, the dissolution of the PU structure with char near 450°C, causes weight loss in all foams [92]. In the NCO-based RPUFs containing EG, these all degradations occurred at the temperature of 303°C, 340°C, and 455°C, respectively, which is depicted in **Figure 32**. The comparison of results of RPUFs based on UCO, NCO, and typical RPUFs is presented in **Table 3**.

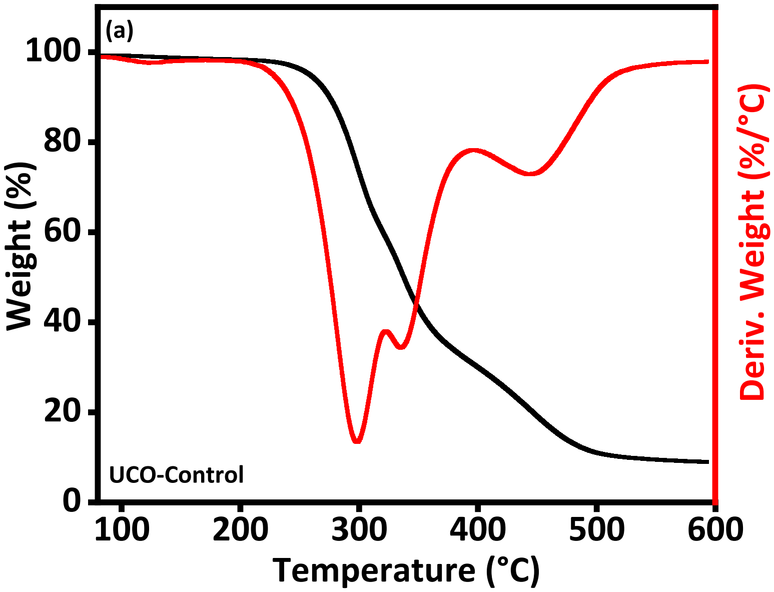

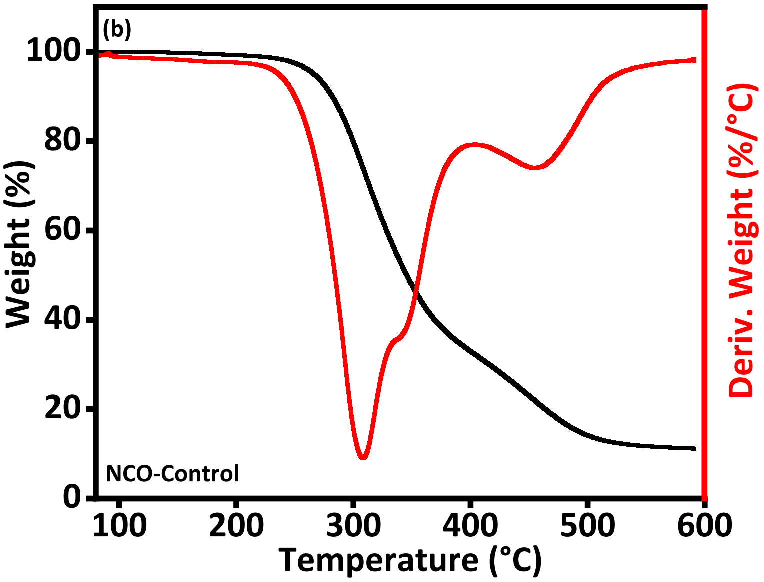

Figure 28. TGA and DTGA curves of **(a)** UCO-Control and **(b)** NCO-Control.

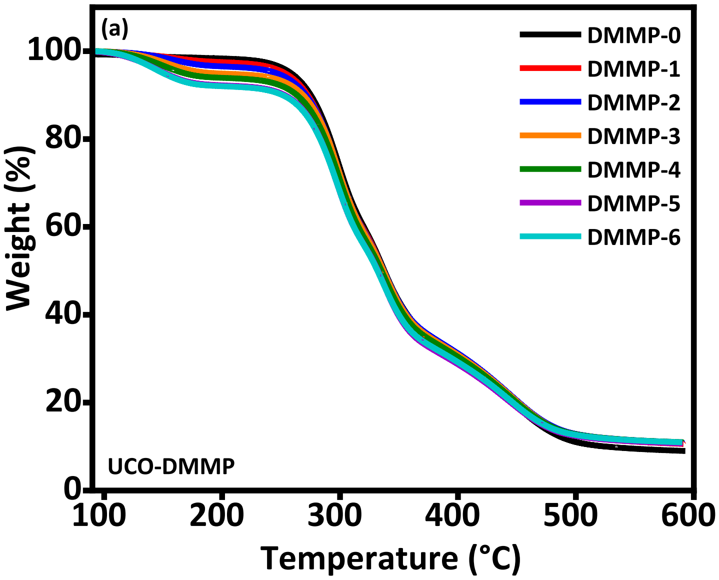

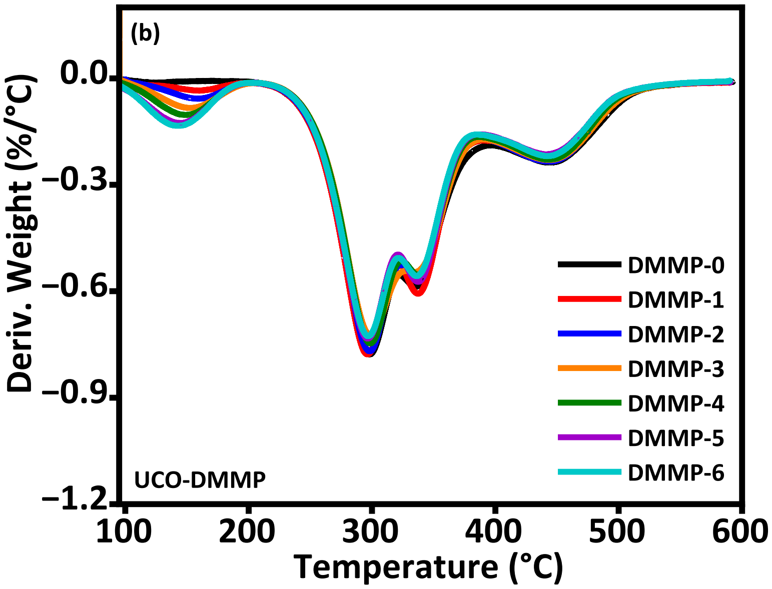

Figure 29. (a) TGA and **(b)** DTGA curves of RPUFs based on UCO with varying amounts of DMMP.

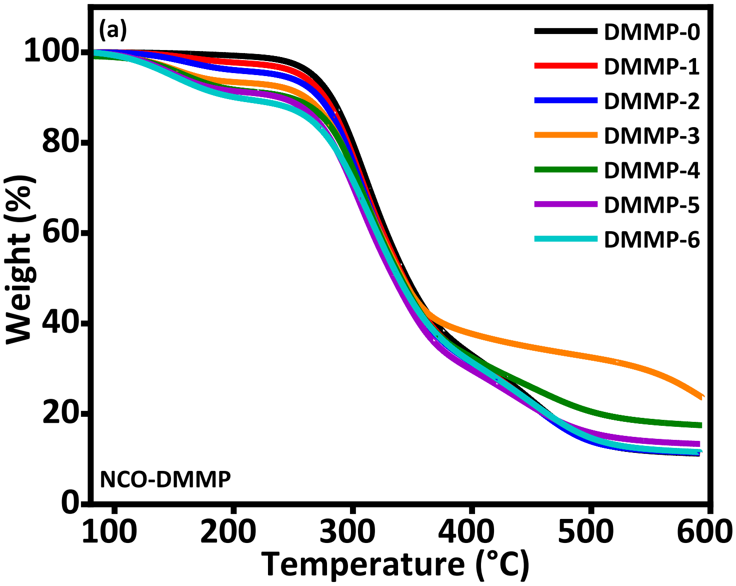

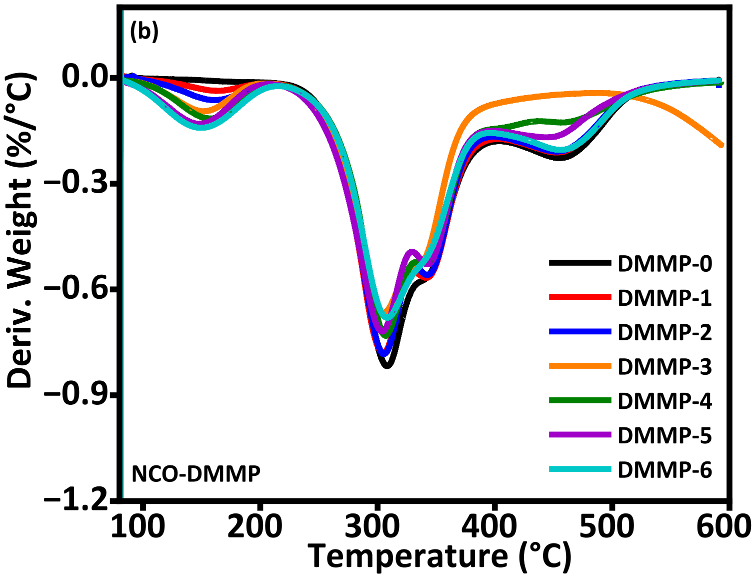

Figure 30. **(a)** TGA and **(b)** DTGA curves of RPUFs based on NCO with varying amounts of DMMP.

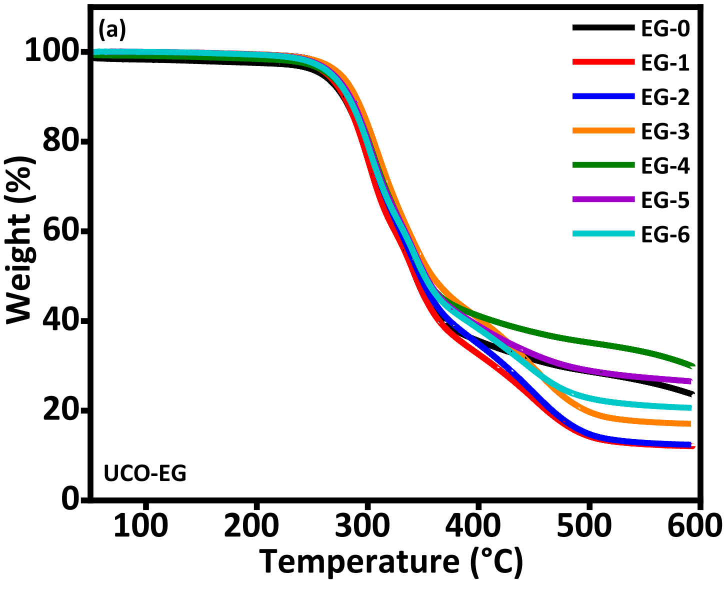

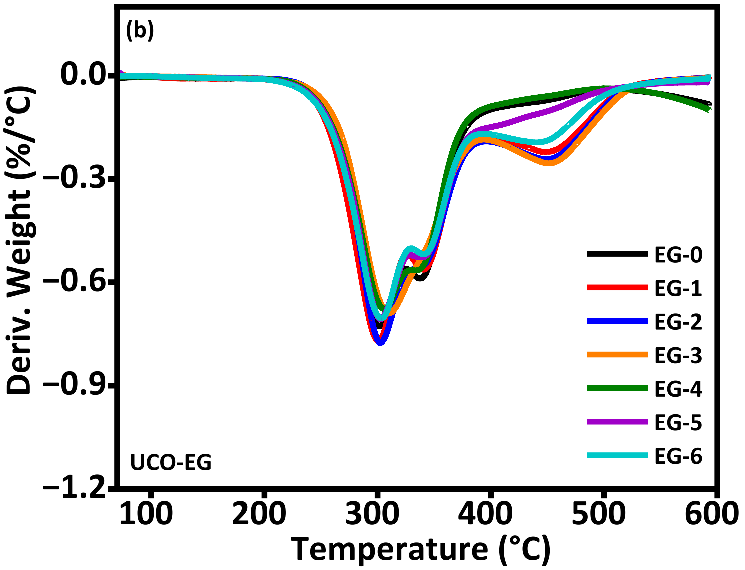

Figure 31. (a) TGA and **(b)** DTGA curves of RPUFs based on UCO with varying amounts of EG.

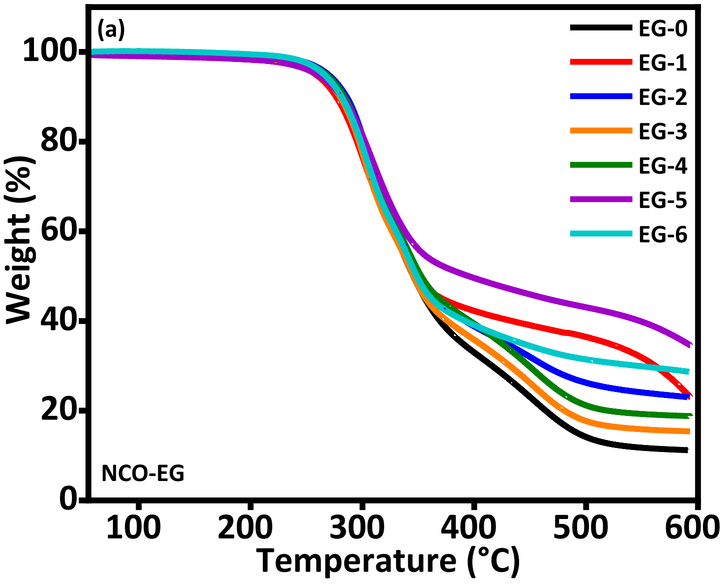

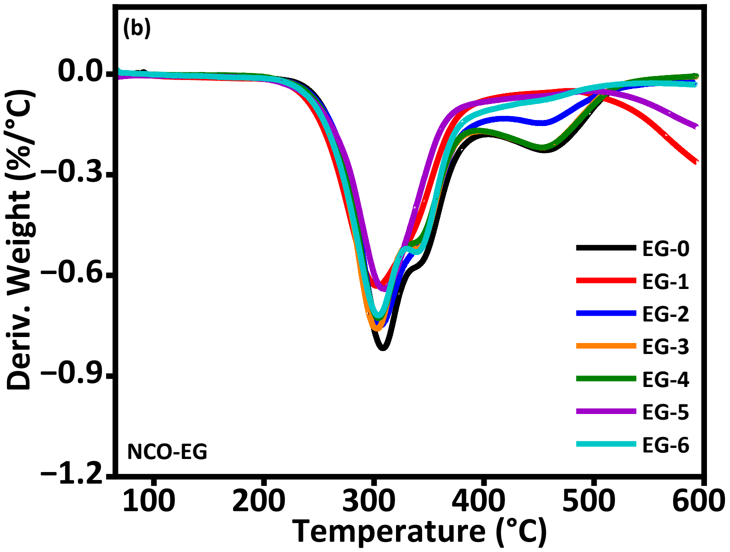

Figure 32. (a) TGA and **(b)** DTGA curves of RPUFs based on NCO with varying amounts of DMMP.

Table 3. Comparison between the results of RPUFs based on UCO, NCO, and typical RPUFs.

		UCO-RPUFs	**NCO-RPUFs**	**Typical RPUFs**	**Ref**
Density (kg/m^3)		38.71	38.88	20-50	[95]
Closed-cell Content (%)		94.64	94.84	95%	[100]
Compression Strength (kPa)		250	270	150-250	[100]
TGA (°C)	1)	220-320	230-330	88-240	[101]
	2)	320-395	330-400	240-395	
	3)	395-515	400-520	395-525	
SEM (µm)		170	167	221	[102]

3.2.6. Horizontal Burning Test

This test provided a visual representation of how the chosen two flame retardants, which are non-halogenated, affected the fire-defense mechanisms of the UCO and NCO-based PU foams. The horizontal burning test method was employed to evaluate the flame-retardant qualities of RPUFs containing DMMP and EG. Fire was given out for ten seconds while the foams were in the horizontal direction. The foam's flame duration and weight loss were recorded after the fire was self-extinguished.

In the absence of flame retardant, RPUFs synthesized using UCO took a total of 54.9 seconds for the fire to completely burn out with a weight loss of 55.24%, whereas RPUFs based on NCO had a burning time of 61 seconds and weight loss of 59.53%. On the other hand, introducing FR in higher quantities resulted in a noticeable decrease in the flame area. The weight loss and burning time of RPUFs treated with EG are displayed in **Figure 33**. The UCO-RPUFs' burning time was significantly reduced by 16.5 seconds after the addition of 6 g of EG as illustrated in **Figure 33(a)**. This foam dropped almost 5.86% of its total weight. The foam that was created with NCO-polyol had a burning time of 15.2 seconds and a weight loss of 6.47% as displayed in **Figure 33(b)**. Images of the foams before and after flaming can be directly associated with the burning time and the percentage of weight lost under the impact of EG: just a very small portion of the foams ignite. This demonstrates the ability of EG to resist flames. These results indicate a significant reduction in the ignition time and weight loss with the increasing volume of EG. It is a graphite compound that contains sulfuric acid intercalated between its carbon layers. When EG is exposed to a heat source, it can react with sulfuric acid instantaneously to produce CO_2, SO_2, and H_2O. This process causes EG to expand enormously at high temperatures for diluting oxygen, which contributes significantly to the gas phase flame retardant. Moreover, the RPUF foam's surface is covered with a "worm-like" char layer formed by the immediate expansion of graphite layers caused by these gases. This layer limits the diffusion of oxygen into the RPUF matrix as well as the spread of combustible volatile products toward the flame zone during combustion and prevents heat transfer. The application of the combined flame-retardant functions of the gas and condensed phases stops the further deterioration of RPUF [97][103]. **Figures 34** and **35** display the images of the UCO-EG and NCO-EG-based RPUFs after burning, respectively.

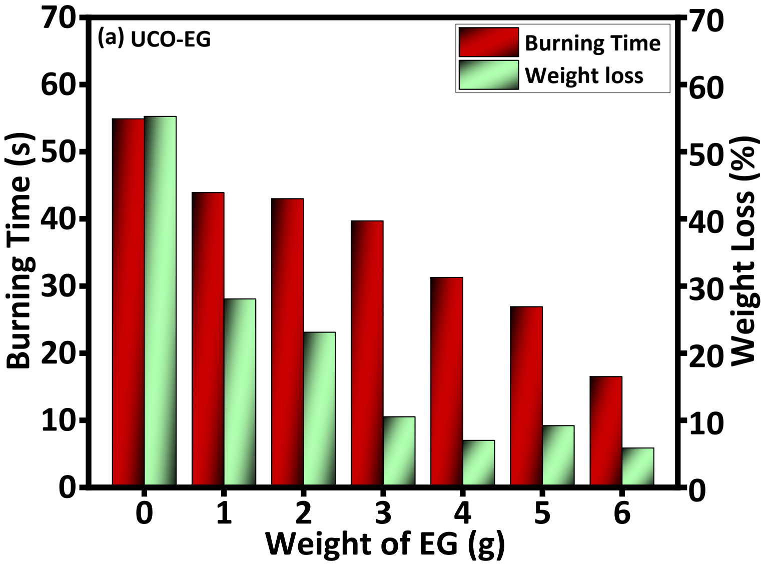

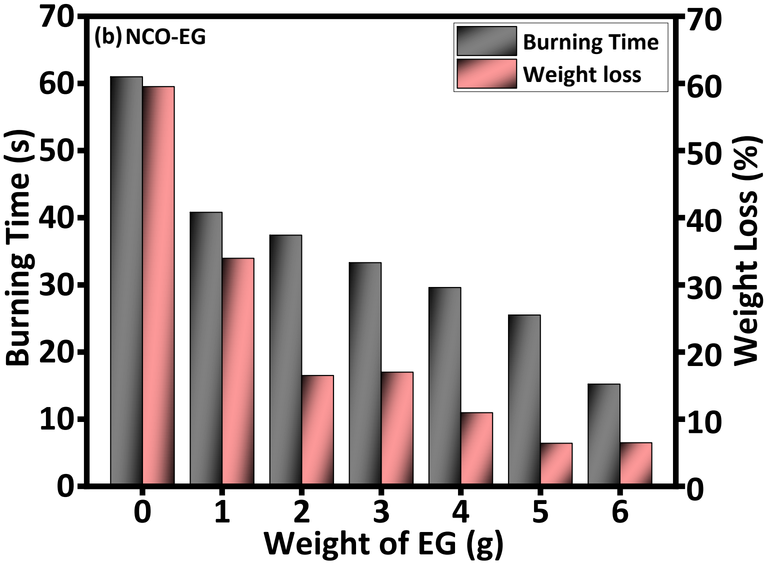

Figure 33. Burning time and weight loss of RPUFs based on **(a)** UCO-EG and **(b)** NCO-EG.

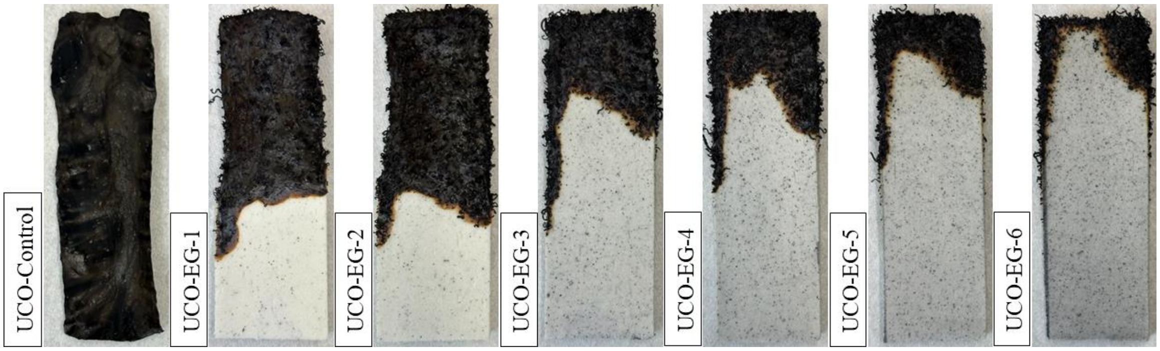

Figure 34. Images of UCO-EG based RPUFs after the burning.

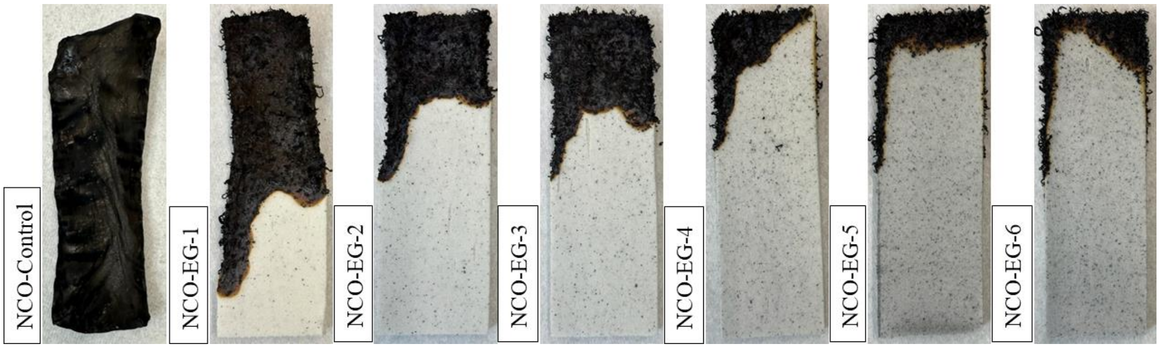

Figure 35. Images of NCO-EG based RPUFs after the burning.

The rigid PU foams treated with DMMP also displayed a considerable improvement in fire-retardant ability along with reducing weight loss, as shown in **Figure 36**. The UCO-based foam containing 1 g of DMMP had a burning time of 30.4 seconds and 27.12% weight loss, which is seen in **Figure 36 (a)**. 28.7 seconds of burning time and 26.32% weight loss were noticed in the NCO-DMMP-1, which was decreased along with the higher amount of DMMP (**Figure 36 (b)**). The lowest flame time of 8.3 seconds and weight loss of 12.10% were recorded in UCO-DMMP-6, while in NCO-DMMP-6, this result was 6.4 seconds and 10.68%, respectively. The images of the UCO-DMMP and NCO-DMMP based RPUFs after the burning are illustrated in **Figures 37** and **38**, respectively.

The notable enhancement in flame resistance was attributed to the dual action of DMMP, both in its condensed and gas phases. Initially, DMMP facilitated the creation of an intumescent protective layer of char on the foam's surface, hindering the spread of oxygen and thermal energy, thus preventing combustion. Additionally, radical phosphorus species like PO*, and PO_2* aided in suppressing the formation of highly reactive radicals H* and OH* [93,99]. The degradation route of the DMMP to form PO* and PO_2* radicals is shown in **Figure 39**. Consequently, it was found that just a small quantity of DMMP was quite successful in making highly flame-retardant PU foams. **Figure 40** represents the general flame-retardant mechanism of DMMP and EG.

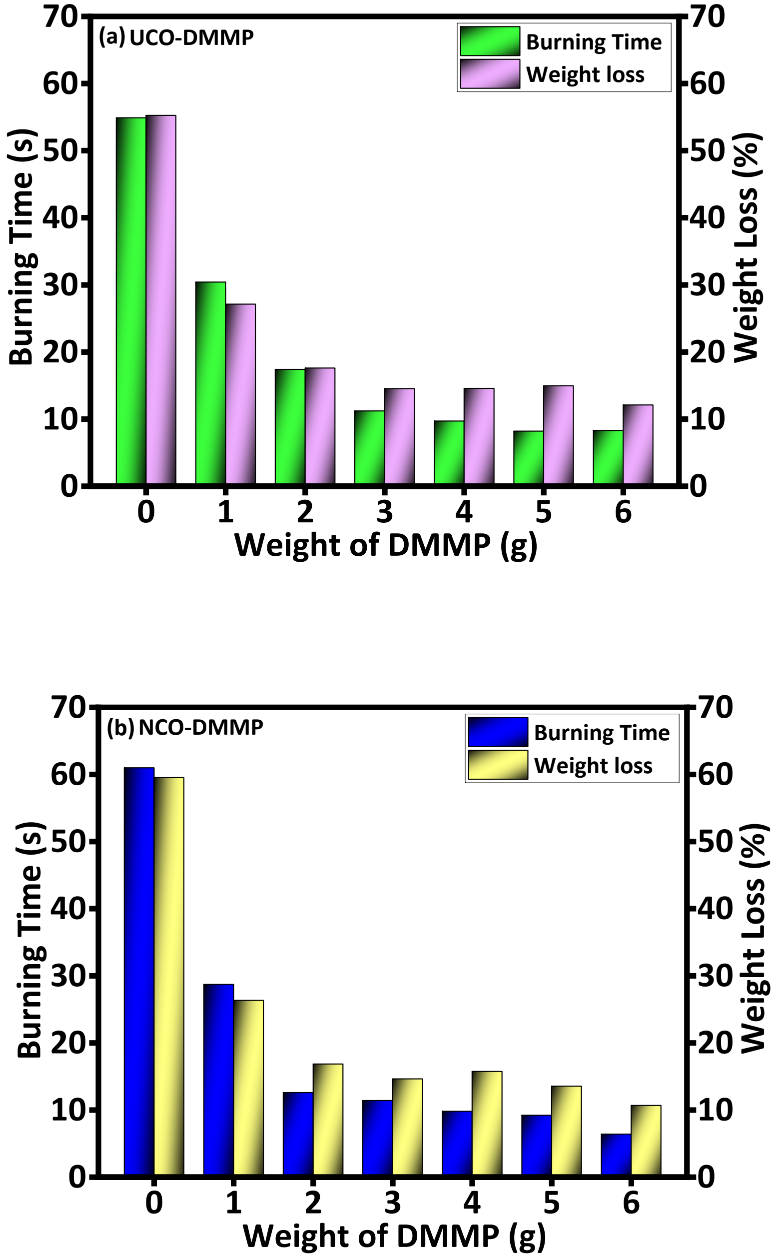

Figure 36. Burning time and weight loss of RPUFs based on **(a)** UCO-DMMP and **(b)** NCO-DMMP.

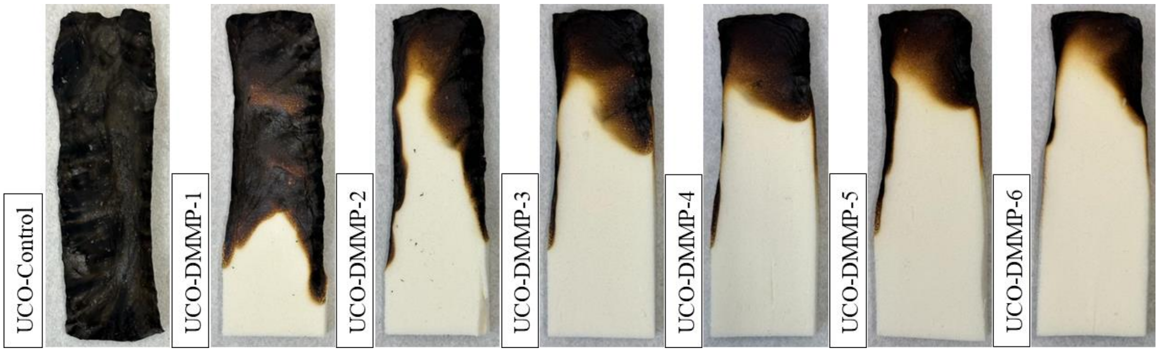

Figure 37. Images of UCO-DMMP based RPUFs after the burning.

Figure 38. Images of NCO-DMMP based RPUFs after the burning.

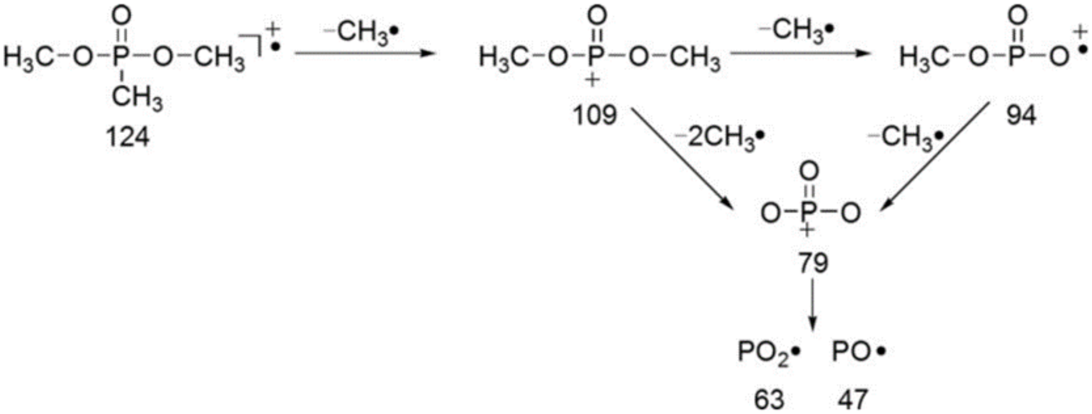

Figure 39. Degradation route of DMMP. Reproduced with permission [98]. Copyright 2013, Wiley.

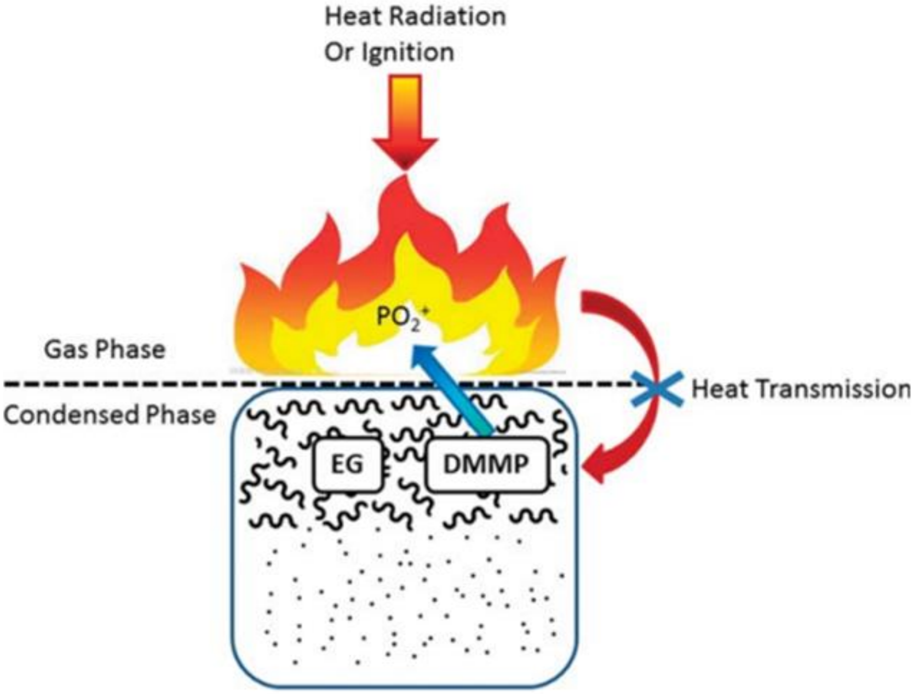

Figure 40. Flame-retardant mechanism of DMMP and EG. Reproduced with permission [98]. Copyright 2013, Wiley.

CHAPTER IV

CONCLUSIONS

The search for affordable and sustainable raw materials for polymers is crucial. This study examined the potential of used canola oil as a beginning resource to produce a reactive polyol, which is essential for the manufacture of RPUF. The epoxidation and ring-opening reaction with methanol to synthesize a bio-based polyol was facilitated by the unsaturated bonds present in the structure of canola oil. This synthetic polyol was utilized to create RPUFs as an environmentally friendly alternative to petroleum-based polyol. The UCO polyol had been determined appropriate for the foam reaction following confirmatory tests such as iodine value, hydroxyl number, FT-IR, and many others. The characterization data of the UCO and the NCO-based polyol are comparable, making the UCO suitable for polyol production. Variable concentrations of non-halogenated flame retardants, such as EG, and DMMP were added to the foaming process of PU foams to mitigate the flammability linked to rigid PU foams. Overall, there was a rise in the assessed properties of the foams.

The density of the foams in EG and DMMP ranged from 38 to 53 kg/m^3, and 32 to 38 kg/m^3, respectively. These ranges are appropriate for a wide range of rigid foam applications in insulation and other commercial uses. There was an overall enhancement in its thermal characteristics and flame retardancy due to the high closed-cell content exceeding 90%. Comparing the rigid foams to those in the literature, they nonetheless attained acceptable outcomes despite the fluctuations in their compression strength of RPUFs that contained EG and the decrease in the foams treated with DMMP. Based on SEM imaging, the mechanical characteristics of the RPUFs are impacted because of increasing and decreasing the foams' cell size with the higher loading of DMMP and EG, respectively. Finally, the burning time for the neat foam was reduced from 54.9 seconds to 16.5 seconds in UCO-EG-6 and 8.3 seconds in UCO-DMMP-6, with a corresponding weight loss of 5.86% and 12.10%. This illustrates a significant improvement in fire retardancy. All these outcomes are similar to those of RPUFs based on NCO. Therefore, it seems appropriate to make use of UCO in the creation of RPUFs based on the similarities in the results of the physical and mechanical properties of the foams. This thesis offers a simple and efficient method for generating biobased RPUF using non-halogenated flame-retardant materials. All these points indicate the possibility of this material being easily applied in large-scale processing shortly.

CHAPTER V

FUTURE SUGGESTIONS

a) Evaluate the cost-effectiveness of utilizing UCO and a comparison of that data with the price of using NCO.

b) Adding both FRs (EG and DMMP) simultaneously to see how they affect the RPUFs' flame-retardancy as well as their mechanical and physical characteristics.

c) Reactive FRs could be introduced rather than additive FRs (EG and DMMP) to observe how they influence the qualities of RPUFs.

d) Recycle these synthetic foams to make polyol from them, which will be further used to create RPUFs. Then, by undertaking several tests, compare these RPUF properties with the previously noted properties.

REFERENCES

[1] X. Li, J. Li, J. Wang, J. Yuan, F. Jiang, X. Yu, F. Xiao, Recent applications and developments of Polyurethane materials in pavement engineering, Constr. Build. Mater. 304 (2021) 124639.

[2] M.F. Sonnenschein, Polyurethanes: Science, Technology, Markets, and Trends, 1st ed., John Wiley & Sons, Inc., MI, USA, 2015.

[3] M. Charlon, B. Heinrich, Y. Matter, E. Couzigné, B. Donnio, L. Avérous, Synthesis, structure and properties of fully biobased thermoplastic polyurethanes, obtained from a diisocyanate based on modified dimer fatty acids, and different renewable diols, Eur. Polym. J. 61 (2014) 197–205.

[4] N. V Gama, A. Ferreira, A. Barros-Timmons, Polyurethane foams: Past, present, and future, Materials (Basel). 11 (2018) 1841.

[5] D.K. Chattopadhyay, K.V.S.N. Raju, Structural engineering of polyurethane coatings for high performance applications, Prog. Polym. Sci. 32 (2007) 352–418.

[6] E. Sharmin, F. Zafar, Chapter 1 :Polyurethane: An Introduction, Polyurethane. (2012) 1–14.

[7] M. Borowicz, J. Paciorek-Sadowska, M. Isbrandt, Synthesis and application of new bio-polyols based on mustard oil for the production of selected polyurethane materials, Ind. Crops Prod. 155 (2020) 112831.

[8] C.T. Pham, B.T. Nguyen, H.T.T. Nguyen, S.J. Kang, J. Kim, P.C. Lee, D.Q. Hoang, Comprehensive Investigation of the Behavior of Polyurethane Foams Based on Conventional Polyol and Oligo-Ester-Ether-Diol from Waste Poly(ethylene terephthalate): Fireproof Performances, Thermal Stabilities, and Physicomechanical Properties, ACS Omega. 5 (2020) 33053–33063.

[9] N.N.P. Nik Pauzi, R. A. Majid, M.H. Dzulkifli, M.Y. Yahya, Development of rigid bio-based polyurethane foam reinforced with nanoclay, Compos. Part B Eng. 67 (2014) 521–526.

[10] J.H. Jang, J.H. Ha, I. Kim, J.H. Baik, S.C. Hong, Facile Room-Temperature Preparation of Flexible Polyurethane Foams from Carbon Dioxide Based Poly(ether carbonate) Polyols with a Reduced Generation of Acetaldehyde, ACS Omega. 4 (2019) 7944–7952.

[11] G.T. Howard, Biodegradation of polyurethane: a review, Int. Biodeterior. Biodegradation. 49 (2002) 245–252.

[12] B. Nohra, L. Candy, J.F. Blanco, C. Guerin, Y. Raoul, Z. Mouloungui, From petrochemical polyurethanes to biobased polyhydroxyurethanes, Macromolecules. 46 (2013) 3771–3792.

[13] R.K. Gupta, P.K. Kahol, eds., Polyurethane Chemistry: Renewable Polyols and Isocyanates, 1st ed., American Chemical Society, Washington, DC, 2021.

[14] N. V. Gama, R. Silva, M. Costa, A. Barros-Timmons, A. Ferreira, Statistical evaluation of the effect of formulation on the properties of crude glycerol polyurethane foams, Polym. Test. 56 (2016) 200–206.

[15] T.A.P. Hai, M. Tessman, N. Neelakantan, A.A. Samoylov, Y. Ito, B.S. Rajput, N. Pourahmady, M.D. Burkart, Renewable polyurethanes from sustainable biological precursors, Biomacromolecules. 22 (2021) 1770–1794.

[16] J.O. Akindoyo, M.D.H. Beg, S. Ghazali, M.R. Islam, N. Jeyaratnam, A.R. Yuvaraj, Polyurethane types, synthesis and applications-a review, RSC Adv. 6 (2016) 114453–114482.

[17] N. Polyurethane, E. Delebecq, J. Pascault, B. Boutevin, U. De Lyon, On the Versatility of Urethane / Urea Bonds : Reversibility , Blocked, (2013).

[18] Z. Petrovic, Polyurethanes from Vegetable Oils, Polym. Rev. 48 (2008) 109.

[19] P. Cinelli, I. Anguillesi, A. Lazzeri, Green synthesis of flexible polyurethane foams from liquefied lignin, Eur. Polym. J. 49 (2013) 1174–1184.

[20] T. Romaskevic, S. Budriene, K. Pielichowski, J. Pielichowski, Application of polyurethane-based materials for immobilization of enzymes and cells: a review, Chemija. 17 (2006) 74–89.

[21] M.A. Izquierdo, F.J. Navarro, F.J. Martínez-Boza, C. Gallegos, Bituminous polyurethane foams for building applications: Influence of bitumen hardness, Constr. Build. Mater. 30 (2012) 706–713.

[22] N.F. Enderus, S.M. Tahir, Green waste cooking oil-based rigid polyurethane foam, IOP Conf. Ser. Mater. Sci. Eng. 271 (2017) 012062.

[23] C.L.P. Vinı´cius B. Veronese, Rodrigo K. Menger, Maria Madalena de C. Forte, Rigid Polyurethane Foam Based on Modified Vegetable Oil, Wiley Online Libr. (2010).

[24] M.R. Islam, M.D.H. Beg, S.S. Jamari, Development of vegetable-oil-based polymers, J. Appl. Polym. Sci. 131 (2014) 9016–9028.

[25] M. Heinen, A.E. Gerbase, C.L. Petzhold, Vegetable oil-based rigid polyurethanes and phosphorylated flame-retardants derived from epoxydized soybean oil, Polym. Degrad. Stab. 108 (2014) 76–86.

[26] F.M. de Souza, P.K. Kahol, R.K. Gupta, Polyols from Sustainable Resources, in: R.K. Gupta, P.K. Kahol (Eds.), Polyurethane Chem. Renew. Polyols Isocyanates, American Chemical Society, Washington, D.C., 2021: pp. 2–25.

[27] M.A. Asare, F.M. de Souza, R.K. Gupta, Natural Resources for Polyurethanes Industries, in: Ram K. Gupta (Ed.), Spec. Polym. Fundam. Prop. Appl. Adv., CRC Press, Boca Raton, FL, 2023.

[28] F.M. de Souza, P.K. Kahol, R.K. Gupta, Biomass-Derived Polyurethanes for Sustainable Future BT - Advances in Green Synthesis: Avenues and Sustainability, in: Inamuddin, R. Boddula, M.I. Ahamed, A. Khan (Eds.), Adv. Green Synth., Springer International Publishing, Cham, Switzerland, 2021: pp. 1–22.

[29] M.Z. Arniza, S.S. Hoong, Z. Idris, S.K. Yeong, H.A. Hassan, A.K. Din, Y.M. Choo, Synthesis of transesterified palm olein-based polyol and rigid polyurethanes from this polyol, J. Am. Oil Chem. Soc. 92 (2015) 243–255.

[30] S.T. McKenna, T.R. Hull, The fire toxicity of polyurethane foams, Fire Sci. Rev. 5 (2016).

[31] A. Bîrca, O. Gherasim, V. Grumezescu, A.M. Grumezescu, Introduction in thermoplastic and thermosetting polymers, Mater. Biomed. Eng. Thermoset Thermoplast. Polym. (2019) 1–28.

[32] J. Massy, Thermoplastic and Thermosetting Polymers, SpringerBriefs Mater. (2017) 19–26.

[33] L. Cong, F. Yang, G. Guo, M. Ren, J. Shi, L. Tan, The use of polyurethane for asphalt pavement engineering applications: A state-of-the-art review, Constr.

Build. Mater. 225 (2019) 1012–1025.
[34] A.J. Raychura, S. Jauhari, V.S. Prajapati, B.Z. Dholakiya, Synthesis and performance evaluation of vegetable oil based wood finish polyurethane coating, Bioresour. Technol. Reports. 3 (2018) 88–94.
[35] P. Li, Y.B. Guo, M.W. Zhou, V.P.W. Shim, Response of anisotropic polyurethane foam to compression at different loading angles and strain rates, Int. J. Impact Eng. 127 (2019) 154–168.
[36] S. Demirel, B. Ergun Tuna, Evaluation of the cyclic fatigue performance of polyurethane foam in different density and category, Polym. Test. 76 (2019) 146–153.
[37] W. Xi, L. Qian, Z. Huang, Y. Cao, L. Li, Continuous flame-retardant actions of two phosphate esters with expandable graphite in rigid polyurethane foams, Polym. Degrad. Stab. 130 (2016) 97–102.
[38] R.K. Gupta, ed., Materials and Chemistry of Flame-Retardant Polyurethanes Volume 2: Green Flame Retardants, 1st ed., American Chemical Society, Washington, DC, 2021.
[39] R.K. Gupta, ed., Materials and Chemistry of Flame-Retardant Polyurethanes Volume 1: A Fundamental Approach, 1st ed., American Chemical Society, Washington, DC, 2021.
[40] W. Xi, L. Qian, Y. Chen, J. Wang, X. Liu, Addition flame-retardant behaviors of expandable graphite and [bis(2-hydroxyethyl)amino]-methyl-phosphonic acid dimethyl ester in rigid polyurethane foams, Polym. Degrad. Stab. 122 (2015) 36–43.
[41] G.E. Hartzell, Overview of combustion toxicology, Toxicology. 115 (1996) 7–23.
[42] X. Liu, J.J.-W. Hao, S. Gaan, Recent studies on the decomposition and strategies of smoke and toxicity suppression for polyurethane based materials, Royal Society of Chemistry, 2016.
[43] P. Carty, Smoke / Char Relationships in PVC Formulations, 13 (1994) 289–299.
[44] S. V. Levchik, E.D. Weil, Thermal decomposition, combustion and fire-retardancy of polyurethanes - A review of the recent literature, Polym. Int. 53 (2004) 1585–1610.
[45] P. Alagi, S.C. Hong, Vegetable oil-based polyols for sustainable polyurethanes, Macromol. Res. 23 (2015) 1079–1086.
[46] A. Prociak, M. Kurañska, E. Malewska, L. Szczepkowski, M. Zieleniewska, J. Ryszkowska, J. Ficon, A. Rzasa, Biobased polyurethane foams modified with natural fillers, Polimery. 60 (2015) 592–599.
[47] J. Jeong, W.S. Kim, M.W. Lee, M. Goh, Liquefaction of Lignin Using Chemical Decomposition and Its Application to Polyurethane Foam, ACS Omega. 6 (2021) 10745–10751.
[48] P. Alagi, Y.J. Choi, S.C. Hong, Preparation of vegetable oil-based polyols with controlled hydroxyl functionalities for thermoplastic polyurethane, Eur. Polym. J. 78 (2016) 46–60.
[49] T. Gurunathan, S. Mohanty, S.K. Nayak, Effect of reactive organoclay on physicochemical properties of vegetable oil-based waterborne polyurethane nanocomposites, RSC Adv. 5 (2015) 11524–11533.
[50] L.C. Bailosky, L.M. Bender, D. Bode, R.A. Choudhery, G.P. Craun, K.J. Gardner,

C.R. Michalski, J.T. Rademacher, G.J. Stella, D.J. Telford, Synthesis of polyether polyols with epoxidized soy bean oil, Prog. Org. Coatings. 76 (2013) 1712–1719.

[51] R.B. Fox, E. Bard, Mechanically Frothed Gel Elastomers and Methods of Making and Using Them, 1 (2015).

[52] D. V. Dounis, G.L. Wilkes, Structure-property relationships of flexible polyurethane foams, Polymer (Guildf). 38 (1997) 2819–2828.

[53] M.A. Asare, F.M. de Souza, R.K. Gupta, Waste to Resource: Synthesis of Polyurethanes from Waste Cooking Oil, Ind. Eng. Chem. Res. 61 (2022) 18400.

[54] W.N.A.W. Azahar, M. Bujang, R.P. Jaya, M.R. Hainin, A. Mohamed, N. Ngadi, D.S. Jayanti, The potential of waste cooking oil as bio-asphalt for alternative binder – An overview, J. Teknol. 78 (2016) 111–116.

[55] S. Srivastava, M. Singh, J. George, K. Bhui, A. Murari Saxena, Y. Shukla, Genotoxic and carcinogenic risks associated with the dietary consumption of repeatedly heated coconut oil, Br. J. Nutr. 104 (2010) 1343–1352.

[56] H. Janik, M. Sienkiewicz, J. Kucinska-Lipka, Polyurethanes, 2014.

[57] A. Konig, U. Fehrenbacher, T. Hirth, E. Kroke, Flexible Polyurethane Foam with the Flame-retardant Melamine, J. Cell. Plast. 44 (2008) 469–480.

[58] J. Diani, K. Gall, Finite Strain 3D Thermoviscoelastic Constitutive Model, Society. (2006) 1–10.

[59] A.M. Palve, J.S. Suroshe, R.K. Gupta, Recent Developments in Nitrogen- and Phosphorous-Based Flame Retardants for Polyurethanes, in: Mater. Chem. Flame-Retardant Polyurethanes Vol. 2 Green Flame Retard., American Chemical Society, 2021: pp. 11–189.

[60] F.M. de Souza, S. Hong, T.A. Nguyen, R.K. Gupta, Aluminum hypophosphite–based highly flame-retardant rigid polyurethanes for industrial applications, in: S. Kanwar, A. Kumar, T.A. Nguyen, S. Sharma, Y. Slimani (Eds.), Biopolym. Nanomater., Elsevier, 2021: pp. 597–614.

[61] F.M. de Souza, R.K. Gupta, Nitrogen-based green flame retardants for bio-polyurethanes, in: S. Kanwar, A. Kumar, T.A. Nguyen, S. Sharma, Y. Slimani (Eds.), Biopolym. Nanomater., Elsevier, 2021: pp. 469–497.

[62] F.M. de Souza, M. Arnce, R.K. Gupta, Enhanced synergistic effect by pairing novel inherent flame-retardant polyurethane foams with nanolayers of expandable graphite for their applications in automobile industry, in: H. Song, T. Nguyen, G. Yasin, N. Singh, R. Gupta (Eds.), Nanotechnol. Automot. Ind., Elsevier, Amsterdam, Netherlands, 2022.

[63] N. Arastehnejad, F. De Souza, R.K. Gupta, Highly flame-retardant and efficient bio-based polyurethane foams via addition of melamine-based intumescent flame-retardants, in: S. Kanwar, A. Kumar, T.A. Nguyen, S. Sharma, Y. Slimani (Eds.), Biopolym. Nanomater., Elsevier, 2021: pp. 497–515.

[64] A.M. Palve, O. V Vani, R.K. Gupta, Metal Oxide-Based Compounds as Flame Retardants for Polyurethanes, in: Mater. Chem. Flame-Retardant Polyurethanes Vol. 2 Green Flame Retard., American Chemical Society, 2021: pp. 121-136 SE–8.

[65] F.M. de Souza, R.K. Gupta, P.K. Kahol, Recent Development on Flame Retardants for Polyurethanes, in: R.K. Gupta, P.K. Kahol (Eds.), Polyurethane Chem. Renew. Polyols Isocyanates, American Chemical Society, Washington, 2021: pp. 187–223.

[66] F.M. de Souza, M. Arnce, R.K. Gupta, F.M. de Souza, M. Arnce, R.K. Gupta, Enhanced synergistic effect by pairing novel inherent flame-retardant polyurethane foams with nanolayers of expandable graphite for their applications in automobile industry, in: H. Song, T. Nguyen, G. Yasin, N. Singh, R. Gupta (Eds.), Nanotechnol. Automot. Ind., Elsevier, Amsterdam, Netherlands, 2022: pp. 65–84.

[67] N. Arastehnejad, M.R. Sulaiman, R.K. Gupta, Nitrogen-Based Ecofriendly Flame Retardants for Polyurethane Foams, in: R.K. Gupta, P.K. Kahol (Eds.), Polyurethane Chem. Renew. Polyols Isocyanates, American Chemical Society, Washington, D.C., 2021: pp. 167–185.

[68] M.A. Asare, F.M. de Souza, V.D. Suthar, R.K. Gupta, Nanocomposite-based flame-retardant polyurethane foams, in: N. Ali, M. Bilal, A. Khan, T.A. Nguyen, R.K. Gupta (Eds.), Smart Polym. Nanocomposites Des. Synth. Funct. Prop. Appl., Elsevier, Amsterdam, Netherlands, 2023: pp. 543–565. https://www.elsevier.com/books/smart-polymer-nanocomposites/ali/978-0-323-91611-0.

[69] K.A. Salmeia, J. Fage, S. Liang, S. Gaan, An overview of mode of action and analytical methods for evaluation of gas phase activities of flame retardants, Polymers (Basel). 7 (2015) 504–526.

[70] J.W. Mitchell, The History and Future Trends of Non-Halogenated Flame Retarded Polymers, John Wiley & Sons, Inc., Beverly, USA, USA, 2014.

[71] F. Laoutid, L. Bonnaud, M. Alexandre, J.M. Lopez-Cuesta, P. Dubois, New prospects in flame retardant polymer materials: From fundamentals to nanocomposites, Mater. Sci. Eng. R Reports. 63 (2009) 100–125.

[72] A.M. Al-Attar, I.M. Abu Zeid, L.F. Felemban, A.M. Shaikh Omar, N.A. Alkenani, Protective and antioxidant effects of chia oil and canola oil on testicular injury induced by lead in rats, J. King Saud Univ. - Sci. 35 (2023) 102894.

[73] Y. Tian, Y. Zhou, M. Kriisa, M. Anderson, O. Laaksonen, M.L. Kütt, M. Föste, M. Korzeniowska, B. Yang, Effects of fermentation and enzymatic treatment on phenolic compounds and soluble proteins in oil press cakes of canola (Brassica napus), Food Chem. 409 (2023) 0–1.

[74] Y. Liu, J. He, R. Yang, Effects of Dimethyl Methylphosphonate, Aluminum Hydroxide, Ammonium Polyphosphate, and Expandable Graphite on the Flame Retardancy and Thermal Properties of Polyisocyanurate-Polyurethane Foams, Ind. Eng. Chem. Res. 54 (2015) 5876–5884.

[75] X. Hu, D. Wang, S. Wang, Synergistic effects of expandable graphite and dimethyl methyl phosphonate on the mechanical properties, fire behavior, and thermal stability of a polyisocyanurate-polyurethane foam, Int. J. Min. Sci. Technol. 23 (2013) 13–20.

[76] Y. Yuan, H. Yang, B. Yu, Y. Shi, W. Wang, L. Song, Y. Hu, Y. Zhang, Phosphorus and Nitrogen-Containing Polyols: Synergistic Effect on the Thermal Property and Flame Retardancy of Rigid Polyurethane Foam Composites, Ind. Eng. Chem. Res. 55 (2016) 10813–10822.

[77] S. Neupane, R.K. Rahman, J. Baker, F. Arafin, E. Ninnemann, K. Thurmond, C.H. Wang, A.E. Masunov, S.S. Vasu, DMMP pyrolysis and oxidation studies at high temperature inside a shock tube using laser absorption measurements of CO, Combust. Flame. 214 (2020) 14–24.

[78] L. Zhang, M. Zhang, Y. Zhou, L. Hu, The study of mechanical behavior and flame retardancy of castor oil phosphate-based rigid polyurethane foam composites containing expanded graphite and triethyl phosphate, Polym. Degrad. Stab. 98 (2013) 2784–2794.
[79] Z. Zhang, D. Li, M. Xu, B. Li, Synthesis of a novel phosphorus and nitrogen-containing flame retardant and its application in rigid polyurethane foam with expandable graphite, Polym. Degrad. Stab. 173 (2020) 109077.
[80] A. Guo, A. Oil, C. Society, P. Examiner, P.D. Niland, United States Patent (19), (2000).
[81] J. Chebet, T. Kinyanjui, P.K. Cheplogoi, Impact of frying on iodine value of vegetable oils before and after deep frying in different types of food in Kenya, J. Sci. Innov. Res. 5 (2016) 193–196.
[82] S. Bhoyate, M. Ionescu, P.K. Kahol, R.K. Gupta, Sustainable flame-retardant polyurethanes using renewable resources, Ind. Crops Prod. 123 (2018) 480–488.
[83] S. Ramanujam, C. Zequine, S. Bhoyate, B. Neria, P. Kahol, R. Gupta, Novel Biobased Polyol Using Corn Oil for Highly Flame-Retardant Polyurethane Foams, C-Journal Carbon Res. 5 (2019) 13.
[84] O. Echeverria-Altuna, O. Ollo, I. Larraza, N. Gabilondo, I. Harismendy, A. Eceiza, Effect of the biobased polyols chemical structure on high performance thermoset polyurethane properties, Polymer (Guildf). 263 (2022) 125515.
[85] M.J. Lerma-García, G. Ramis-Ramos, J.M. Herrero-Martínez, E.F. Simó-Alfonso, Authentication of extra virgin olive oils by Fourier-transform infrared spectroscopy, Food Chem. 118 (2010) 78–83.
[86] M.D. Guillén, N. Cabo, Characterization of edible oils and lard by fourier transform infrared spectroscopy. Relationships between composition and frequency of concrete bands in the fingerprint region, J. Am. Oil Chem. Soc. 74 (1997) 1281–1286.
[87] A.M. Sienkiewicz, P. Czub, The unique activity of catalyst in the epoxidation of soybean oil and following reaction of epoxidized product with bisphenol A, Ind. Crops Prod. 83 (2016) 755–773.
[88] G. Kiss, G. Rusu, G. Bandur, I. Hulka, D. Romecki, F. Péter, Advances in low-density flexible polyurethane foams by optimized incorporation of high amount of recycled polyol, Polymers (Basel). 13 (2021) 1–15.
[89] H. Pawlik, A. Prociak, Influence of Palm Oil-Based Polyol on the Properties of Flexible Polyurethane Foams, J. Polym. Environ. 20 (2012) 438–445.
[90] W. Xing, H. Yuan, P. Zhang, H. Yang, L. Song, Y. Hu, Functionalized lignin for halogen-free flame retardant rigid polyurethane foam: Preparation, thermal stability, fire performance and mechanical properties, J. Polym. Res. 20 (2013) 1–12.
[91] P. Acuña, Z. Li, M. Santiago-Calvo, F. Villafañe, M. ángel Rodríguez-Perez, D.Y. Wang, Influence of the characteristics of expandable graphite on the morphology, thermal properties, fire behaviour and compression performance of a rigid polyurethane foam, Polymers (Basel). 11 (2019) 168.
[92] F. M. de Souza, J. Choi, S. Bhoyate, P.K. Kahol, R.K. Gupta, Expendable Graphite as an Efficient Flame-Retardant for Novel Partial Bio-Based Rigid Polyurethane Foams, C — J. Carbon Res. 6 (2020) 27.

[93] C. Zhang, S. Bhoyate, M. Ionescu, P.K. Kahol, R.K. Gupta, Highly flame retardant and bio-based rigid polyurethane foams derived from orange peel oil, Polym. Eng. Sci. 58 (2018) 2078–2087.

[94] Y.Y. Chan, C. Ma, F. Zhou, Y. Hu, B. Schartel, Flame retardant flexible polyurethane foams based on phosphorous soybean-oil polyol and expandable graphite, Polym. Degrad. Stab. 191 (2021) 109656.

[95] T. Widya, C.W. Macosko, Nanoclay-modified rigid polyurethane foam, J. Macromol. Sci. - Phys. 44 B (2005) 897–908.

[96] L. Liu, Z. Wang, M. Zhu, Flame retardant, mechanical and thermal insulating properties of rigid polyurethane foam modified by nano zirconium amino-tris-(methylenephosphonate) and expandable graphite, Polym. Degrad. Stab. 170 (2019) 108997.

[97] Z. Yang, H. Peng, W. Wang, T. Liu, Crystallization behavior of poly(ε-caprolactone)/layered double hydroxide nanocomposites, J. Appl. Polym. Sci. 116 (2010) 2658–2667.

[98] F. Feng, L. Qian, The flame retardant behaviors and synergistic effect of expandable graphite and dimethyl methylphosphonate in rigid polyurethane foams, Polym. Compos. 35 (2014).

[99] N.M. Barkoula, B. Alcock, N.O. Cabrera, T. Peijs, Flame-Retardancy Properties of Intumescent Ammonium Poly(Phosphate) and Mineral Filler Magnesium Hydroxide in Combination with Graphene, Polym. Polym. Compos. 16 (2008) 101–113.

[100] I. Javni, W. Zhang, Z.S. Petrović, Soybean-oil-based polyisocyanurate rigid foams, J. Polym. Environ. 12 (2004) 123–129.

[101] U. Stirna, A. Fridrihsone, B. Lazdiņa, M. Misāne, D. Vilsone, Biobased Polyurethanes from Rapeseed Oil Polyols: Structure, Mechanical and Thermal Properties, J. Polym. Environ. 21 (2013) 952–962.

[102] F.R. Vieira, N. V. Gama, D. V. Evtuguin, C.O. Amorim, V.S. Amaral, P.C.O.R. Pinto, A. Barros-Timmons, Bio-Based Polyurethane Foams from Kraft Lignin with Improved Fire Resistance, Polymers (Basel). 15 (2023).

[103] W.-Z. Xu, L. Liu, S.-Q. Wang, Y. Hu, Synergistic effect of expandable graphite and aluminum hypophosphite on flame-retardant properties of rigid polyurethane foam, J. Appl. Polym. Sci. 132 (2015).